

**International Series in the Science of the Solid State**  
Volume 12  
Editor: B.R. Pamplin

**OTHER TITLES IN THE SERIES:**

- Volume 1 : GREENAWAY and HARBEKE—Optical Properties and Band Structures of Semiconductors  
Volume 2 : RAY—II-VI Compounds  
Volume 3 : NAG—Theory of Electrical Transport in Semiconductors  
Volume 4 : JARZEBSKI—Oxide Semiconductors  
Volume 5 : SHARMA and PUROHIT—Semiconductor Heterojunctions  
Volume 6 : PAMPLIN—Crystal Growth  
Volume 7 : SHAY and WERNICK—Ternary Chalcopyrite Semiconductors: Growth, Electronic Properties and Applications  
Volume 8 : BASSANI and PASTORI PARRAVICINI—Electronic States and Optical Transitions in Solids  
Volume 9 : SUCHET—Electrical Conduction in Solid Materials. (Physicochemical Bases and Possible Applications)  
Volume 10 : TANNER—X-Ray Diffraction Topography  
Volume 11 : ROY—Tunnelling and Negative Resistance Phenomena in Semiconductors  
Volume 13 : WILLIAMS and HALL—Luminescence and the Light Emitting Diode

*A NEW REVIEW JOURNAL, ALSO OF INTEREST:*

**PROGRESS IN CRYSTAL GROWTH AND CHARACTERIZATION**

Full details of the above titles are available from your nearest Pergamon office on request.

# THERMAL EXPANSION OF CRYSTALS

**R.S. KRISHNAN**  
(Formerly Professor of Physics  
Indian Institute of Science Bangalore)  
VICE-CHANCELLOR, UNIVERSITY OF KERALA  
TRIVANDRUM-695501

**R. SRINIVASAN**  
Professor of Physics  
Indian Institute of Technology  
Madras-600036

and

**S. DEVANARAYANAN**  
Reader, Department of Physics  
University of Kerala, Trivandrum-695581



**PERGAMON PRESS**  
OXFORD · NEW YORK · TORONTO  
SYDNEY · PARIS · FRANKFURT

Pergamon Press Ltd, Headington Hill Hall, Oxford  
OX3 0BW, England

Pergamon Press Inc., Maxwell House, Fairview Park,  
Elmsford, New York 10523, U.S.A.  
Pergamon of Canada, Suite 104, 150 Consumers Road,  
Willowdale, Ontario M2J 1P9, Canada  
Pergamon Press (Aust.) Pty. Ltd., PO Box 544, Potts Point,  
N.S.W. 2011, Australia  
Pergamon Press SARL, 24 rue des Ecoles,  
75240 Paris, Cedex 05, France  
Pergamon Press GmbH, 6242 Kronberg-Taunus,  
Pferdstasse 1, West Germany

Copyright © 1979 Pergamon Press Ltd.

All Rights Reserved. No part of this publication may be reproduced, stored in a retrieval system or transmitted in any form or by any means: electronic, electrostatic, magnetic tape, mechanical photocopying, recording or otherwise, without permission in writing from the publishers

First Edition 1979

#### British Library Cataloguing in Publication Data

Krishnan, R S

Thermal expansion of crystals.—(International series in the science of the solid state; vol. 12).

1. Crystals—Thermal properties 2. Expansion (Heat)

I. Title II. Srinivasan, R III. Devanarayana, S

IV. Series

548.5 QD937

77-30620

ISBN 0-08-021405-3

## Contents

	Page
<b>Preface</b>	vii
<b>1 General Introduction</b>	1
1.1 Introduction	1
1.2 Grüneisen's relation and the second Grüneisen constant	3
1.3 The number of constants in various crystal systems	5
<b>2 Methods of measurement of thermal expansion of solids</b>	6
2.1 Introduction	6
2.2 Microscopic (lattice) measurements	7
2.3 Macroscopic Methods	15
2.4 Recent efforts to standardise thermal expansion measurements	
2.5 Reduction of the observations on thermal expansion	47
<b>3 Theory of thermal expansion of crystals</b>	48
3.1 Lattice contributions to thermal expansion	47
3.2 Calculation of $\alpha_0$	54
3.3 Analysis of experimental data	60
3.4 Electronic and magnetic contribution to thermal expansion	61
3.5 Comparison between theory and experiment	67
3.6 Thermal expansion of Anisotropic materials	69
3.7 Rigorous theory of thermal expansion	91
3.8 Analysis of data at high temperatures	97
3.9 Negative thermal expansion in solids	99
<b>4 Thermal expansion and phase transitions</b>	103
4.1 Relations near a phase transition	105
4.2 Experimental data on ammonium compounds	107
4.3 Thermal expansion and ferroelectricity	111
<b>5 Thermal expansion data</b>	115

548.86  
K89t.

Engin.

Engin 5 May 80

## Contents

5.1 At high temperatures	118
5.2 At very low temperatures	184
Appendix I	195
References	197
Additional References	251
Further References	283
Recent References	289
Appendix II	299
Author Index	301

## Preface

Thermal expansion of a solid is a direct consequence of the anharmonicity of lattice vibrations. It, therefore, provides a convenient measure of the anharmonic parameters in a crystal. The anisotropy of thermal expansion is clearly exhibited if measurements are made on a single crystal. The anisotropy is related to the crystal system.

One meets with a variety of behaviour if the thermal expansion of crystals is studied over a wide temperature range. There are crystals like germanium in which the expansion changes sign twice as the temperature is reduced. There are anisotropic crystals like calcite in which the expansion is positive in one direction and negative in the other.

The simple theory of thermal expansion of crystals given by Grüneisen in 1929 predicted the expansion co-efficient to decrease to zero as the temperature tends to the absolute zero. The expansion coefficient of many crystals near the boiling point of liquid helium is of the order of  $10^{-8}/^{\circ}\text{K}$ . This necessitates new and sensitive experimental techniques to determine the thermal expansion in this temperature range. It was also realised that one should make measurements at low temperatures to detect deviations from the simple Grüneisen theory, arising from the complicated phonon spectrum of the lattice.

In the years from 1960 onwards there has been a spate of work on the thermal expansion of crystals—both theoretical and experimental. On the experimental side, besides the refinements in the existing techniques for lattice and macroscopic expansion measurements, several new sensitive techniques were developed to measure changes as small as  $10^{-8}$  cm in the length of the specimen. Among these techniques mention should be made of the three-terminal capacitance dilatometer, the differential transformer dilatometer and the Fabry-Perot interference dilatometer. Though these and other techniques are described in individual papers in the literature there has been no discussion of the relative merits of these techniques. There has also been a lot of effort at automatic and continuous recording of the dilatation of a specimen as the temperature

is changed. A detailed review of the different experimental techniques with a discussion of the inherent sources of error and methods for their elimination will be of interest to the experimental research worker in this field.

Considerable amount of data on thermal expansion has been collected down to 4.2 K on simple crystals by the painstaking application of one or the other experimental technique mentioned above. These results reveal the possibility of more than one contribution to the thermal expansion of a crystal. These different contributions have different origins and hence different characteristic temperature dependences at low temperatures. For example, the electronic contribution in metals at low temperatures varies linearly with the Absolute temperature and provides information on the volume derivative of the density of states at the Fermi level. The lattice contribution, on the other hand, is proportional to  $T^3$  at low temperatures; and it is related to the pressure derivatives of the second-order elastic constants in these materials. As long as the temperature  $T$  is less than half the Debye temperature, one could use the quasi-harmonic approximation in the theory of thermal expansion. Detailed calculations on rare gas solids, cubic metals, semiconductors and ionic crystals with simple structures have been made and we have now a fair degree of understanding of the temperature variation of linear thermal expansion coefficient in these materials. However, there is a paucity of theoretical work in anisotropic materials. Some ground rules exist for a general explanation of the temperature variation of thermal expansion in these crystals. But we have as yet no sound knowledge of the crystal potential in these materials.

The measurements of thermal expansion at high temperatures almost upto the melting point of some of the cubic materials have provided information on the relative importance of cubic and quartic anharmonic terms which have been omitted in the quasi-harmonic approximation.

Precise measurements of thermal expansion at very low temperatures provide additional data for the  $T = 0$  molar volume (or, lattice parameter) of a substance. This quantity enables interpretation of the van Alphen-de Haas measurements on the substance.

The thermal expansion of a crystal also shows some interesting variations when the crystal undergoes phase transformations. The phase transformation in ammonium halides have been studied with a view to testing the Ehrenfest-Pippard relations. In the case of ferroelectric crystals containing hydrogen bonds, the changes in the thermal expansion coefficients at the ferroelectric transition point are related to the reorientation of the hydrogen bonds.

This book presents a comprehensive review on these various aspects

of thermal expansion. A comparison of the various methods of measurement is made with comments on the relative merits of the different methods. A very detailed review of the theory of thermal expansion is provided with critical comments on the works of various authors. The behaviour of thermal expansion when phase transformations occur, and in ferroelectric materials forms the subject matter of a separate chapter. It is hoped that this review will prove to be of value to the experimental and theoretical workers in this field.

It was also thought desirable to collect all the published data on thermal expansion of about 370 scientifically and technologically important materials (mostly crystals) and to present them for ready reference in the form of tables. The data have been fitted to empirical formulae and the constants in the formulae have been tabulated at high and at low temperatures. These tables can be used with ease.

The value of the book lies also in the comprehensive literature survey that has been done on thermal expansion of solids in general and work related to it which may prove useful for further study. There are more than 1800 references cited at the end of the book, giving the names of authors, journals and titles of papers as appeared in the literature. These references have been brought upto date till the middle of 1977. It is noteworthy that more than 74% of the publications belong to the period from 1960 to 1977. The authors hope that the comprehensive survey of the literature on thermal expansion of solids in general and work related to it presented in this book may prove useful to research workers for further study.

The authors are indebted to Dr. S.V. Subramanyam, Department of Physics, Indian Institute of Science, Bangalore, for his invaluable help in the preparation and checking the correctness of the bibliography listed in the book.

Dated: 1.7.1977

R.S. Krishnan  
R. Srinivasan  
S. Devanarayana

Note added in proof:

The list of electronic materials and the pages on which their thermal expansion data are given are summarized in Appendix II.

The bibliography of papers published on the subject has been brought up to the end of February 1979 and is given under the heading "Recent References" on page 289. The total number now exceeds 2110.

31.5.79.

R. S. Krishnan

## CHAPTER 1

### General Introduction

#### 1.1. INTRODUCTION

The expansion of a crystal when it is heated is a direct manifestation of the anharmonic nature of the interatomic forces in solids. If the forces were purely harmonic the mean positions of the atoms would not change even though the atoms would vibrate with larger and larger amplitudes as the temperature increases. While the temperature variation of the specific heat of solids was quite well understood with the development of the Born-von Karman's theory of lattice vibrations in crystals, there was little attempt to calculate the thermal expansion of crystals in any detail till recently. This was partly because of the paucity of experimental data on the thermal expansion of crystals below room temperature. While Grüneisen's theory of thermal expansion provided a general explanation of the phenomenon on the quasi-harmonic approximation, a detailed study of the temperature variation of thermal expansion below room temperature was started only after the work of Barron (64) in 1955. The theoretical study provided an impetus to the development of refined experimental techniques to measure the thermal expansion of crystals down to liquid helium temperature. The techniques so developed are sensitive enough to measure a change in length of the specimen of a fraction of an Ångström! A large body of reliable data has been accumulated on a variety of simple crystals in which the forces of interaction are fairly well understood. A fairly satisfactory explanation has been provided for the temperature variation of the thermal expansion in these simple solids on the quasi-harmonic theory. This review deals with the progress achieved both in the theoretical and experimental study of thermal expansion in recent times. An exhaustive collection of the data on the thermal expansion of a large variety of crystals has also been made so that the work can be used as a ready reference book.

The *linear thermal expansion coefficient*  $\alpha$  of a solid is defined as the increase in length suffered by unit length of the solid when its temperature

is raised by a degree Celsius. The limiting value of the ratio  $\frac{1}{V} \frac{\delta V}{\delta T}$  as the increase in temperature  $\delta T \rightarrow 0$  is defined as the true expansion coefficient of the solid. Usually it is the mean coefficient of expansion over a temperature range  $\delta T$  that is measured. The smaller this range of temperature the more nearly does the mean coefficient of expansion approach the true coefficient. A similar definition holds for the volume expansion coefficient,  $\beta$ , of the solid. The volume expansion coefficient of the solid is related to its linear expansion coefficient. To a first degree of approximation the volume expansion coefficient is the sum of the linear expansion coefficients in three mutually perpendicular directions in the solid.

Solids can be crystalline or amorphous—an example for the latter being glass. We are concerned only with crystalline solids. These are available in two forms: single crystals formed by the monotonous repetition in space of a simple structural unit according to definite laws of symmetry; or polycrystalline material composed of small crystallites oriented in all possible directions. It is needless to emphasize that for any theory of the solid state a study of single crystals is of great importance. Polycrystalline material introduces great complexities in the understanding of the physical processes involved. As an example, mention may be made of cadmium and zinc where a study of the expansion of polycrystalline material yielded widely divergent results. This confusion was cleared up when single crystals of these substances were studied.

The measurement of thermal expansion of crystals is of importance for the following reasons:

1. The expansion of a crystal is intimately related to the normal modes of vibration of the crystal lattice and hence a study of it might be expected to throw some light on the nature of binding between the different units in the lattice.
2. The expansion coefficient is a structure sensitive property and reflects any transitions in crystal structure.
3. Expansion coefficient values are needed to convert the  $C_p$  values observed in experiments to the  $C_v$  values required by the theory of specific heat. The thermodynamic relation connecting them is given by

$$C_p - C_v = \beta^2 VT / \chi_T \quad (1.1)$$

where  $C_p$  = Molar specific heat at constant pressure of the solid in Cals/°K,

$C_v$  = Molar specific heat at constant volume of the solid in Cals/°K,

$\beta$  = the volume expansion coefficient of the solid,

$V$  = the volume of the solid,

$\chi$  = Compressibility of the solid,  
 $T$  = Temperature of the solid,

and  $J$  = Mechanical equivalent of heat.

4. Precise measurements of thermal expansion at very low temperatures provide additional data for  $T = 0$  molar volume of a substance. A knowledge of this quantity is essential to interpret properly the van Alphen-de Haas measurements on the substance.

5. Knowledge of thermal expansion at low temperatures is useful to isolate the electronic and the nuclear hyperfine contributions to the Grüneisen parameter from the lattice contribution.

6. An extremely useful quantity in physics at high pressures is the *Grüneisen parameter*. Through this parameter maximum information may be extracted from limited data, which is of advantage in experimentally difficult conditions where data are often unobtainable. Thermal expansion data enable evaluation of the Grüneisen parameter.

7. Another quantity of interest in recent years is the *second Grüneisen constant*,  $q$ , which is the first order volume derivative of the normal Grüneisen parameter,  $GP$ . These two quantities,  $q$  and  $GP$ , are fundamental to the study of many basic phenomena in solids and to the prediction of a variety of physical properties like the equation of state.

8. A knowledge of lattice thermal expansion of a material is essential in investigations involving epitaxy and thin film growth and in thin film deposition in industry.

## 1.2. GRÜNEISEN'S RELATION AND SECOND GRÜNEISEN CONSTANT

Grüneisen (415) observed that for a large number of crystalline solids the coefficient of thermal expansion,  $\alpha$ , should be proportional to the specific heat,  $C_v$ , over quite wide ranges of temperatures and even at low temperatures. This statement, known as the "*Grüneisen's rule*", can be expressed in the form

$$\frac{3\alpha}{\chi_T} = \gamma \frac{C_v}{V} \quad (1.2.1)$$

where  $\chi_T$  is the isothermal compressibility of the solid, and  $\gamma$  is a dimensionless quantity, referred to as the *Grüneisen constant*. Grüneisen (415) from early expansion data gave values for the parameter,  $\gamma$ , generally in the vicinity of 2.  $\gamma$  was found to be independent of temperature.

The first-order volume derivative of  $\gamma$  is called the "*second Grüneisen constant*",  $q$ , to distinguish it from the normal Grüneisen parameter. It is expressed in the form

TABLE 1.1.

Crystal System	Axial relations	No. of constants	Thermal expansion tensor referred to axes in the conventional orientation
1. Triclinic	$a \neq b \neq c$ $\alpha \neq \beta \neq \gamma$	6	$\begin{bmatrix} \alpha_{11} & \alpha_{21} & \alpha_{31} \\ \alpha_{21} & \alpha_{22} & \alpha_{32} \\ \alpha_{31} & \alpha_{32} & \alpha_{33} \end{bmatrix}$
2. Monoclinic	$a \neq b \neq c$ $\alpha = \beta = 90^\circ$ $\gamma \neq 90^\circ$	4	$\begin{bmatrix} \alpha_{11} & 0 & \alpha_{31} \\ 0 & \alpha_{22} & 0 \\ \alpha_{31} & 0 & \alpha_{33} \end{bmatrix}$
3. Orthorhombic	$a \neq b \neq c$ $\alpha = \beta = \gamma = 90^\circ$	3	$\begin{bmatrix} \alpha_{11} = \alpha_1 & 0 & 0 \\ 0 & \alpha_{22} = \alpha_2 & 0 \\ 0 & 0 & \alpha_{33} = \alpha_3 \end{bmatrix}$
4. Tetragonal	$a = b \neq c$ $\alpha = \beta = \gamma = 90^\circ$		
5a. Hexagonal (Trigonal)	$a = b = c$ $\alpha = \beta = \gamma \neq 90^\circ$ , $< 120^\circ$	2	$\begin{bmatrix} \alpha_{11} = \alpha_1 & 0 & 0 \\ 0 & \alpha_{22} = \alpha_1 & 0 \\ 0 & 0 & \alpha_{33} = \alpha_3 \end{bmatrix}$
5b. Hexagonal	$a = b \neq c$ $\alpha = \beta = 90^\circ$ , $\gamma = 120^\circ$		
6. Cubic and Isotropic	$a = b = c$ $\alpha = \beta = \gamma = 90^\circ$	1	$\begin{bmatrix} \alpha_{11} = \alpha & 0 & 0 \\ 0 & \alpha_{22} = \alpha & 0 \\ 0 & 0 & \alpha_{33} = \alpha \end{bmatrix}$

(Some authors distinguish, in different ways, an equivalence of the hexagonal system, calling it "trigonal" or "rhombohedral". M.J. Bueger points out in his book on "Contemporary Crystallography" that such practices lead to serious inconsistencies and should be avoided).

$$q = \frac{d \ln \gamma}{d \ln V} \quad (1.2.2)$$

### 1.3. THE NUMBER OF CONSTANTS IN VARIOUS CRYSTAL SYSTEMS

Thermal expansion coefficient,  $\alpha$ , is a second-rank symmetric tensor relating temperature  $T$  (a scalar) and another second-rank tensor  $\epsilon_{ik}$  (strain) by

$$[\epsilon_{ik}] = [\alpha_{ik}] \cdot T \quad (1.3.1)$$

where

$$[\alpha_{ik}] = \begin{bmatrix} \alpha_{11} & \alpha_{21} & \alpha_{31} \\ \alpha_{21} & \alpha_{22} & \alpha_{32} \\ \alpha_{31} & \alpha_{32} & \alpha_{33} \end{bmatrix} \quad (1.3.2)$$

There are six crystal systems and the number of independent constants  $\alpha_{ik}$  of the expansion coefficient depends on the system to which the crystal belongs. The maximum number of independent constants  $\alpha_{ik}$  is six; but this number is reduced for crystals of higher symmetry. Wooster (1962) has deduced the number of constants for various crystal systems in his book on *Crystal Physics*. Accordingly, there are six constants for triclinic crystals, four for monoclinic, three for orthorhombic, two for tetragonal and hexagonal and one for cubic systems. The thermal deformation ellipsoid is a sphere in the cubic system and a spheroid of revolution in the tetragonal and hexagonal systems. In all crystals, except those belonging to the triclinic and monoclinic systems, the principal axes of the ellipsoid coincide with the principal crystallographic axes. In the triclinic and monoclinic crystals, the orientation of the ellipsoid with respect to the crystallographic axes is given by the additional number of constants. This orientation changes with temperature. The non-vanishing tensor components for the six crystal systems are given in Table 1.1.

$$3\alpha = \gamma \frac{C_v \lambda_T}{V} \quad (2.1.1)$$

shows that, for example, with

$$\gamma = 2, \quad V = 10 \text{ cm}^3$$

$$C_v = 1946 \times 10^7 (T/\Theta_D)^3 \text{ erg/gm. mole/}^\circ\text{K, and}$$

$$\lambda_T = 10^{-12} \text{ cm}^2/\text{dyne,}$$

$$\alpha = 1.3 \times 10^{-3} (T/\Theta_D)^3 / ^\circ\text{K} \quad (2.1.2)$$

For  $T/\Theta_D = 0.1$ ,  $\alpha = 10^{-6} / ^\circ\text{K}$ , and

$$T/\Theta_D = 0.01, \alpha = 10^{-9} / ^\circ\text{K}.$$

Thus the sensitivity of measurement required in the region below  $\frac{\Theta_D}{50}$  is of the order of  $10^{-9} / ^\circ\text{K}$ . This result will be referred to later while discussing the merits of the various techniques of measurements.

### 2.1.2. Estimation of Error

The relative error in the measurement of thermal expansion coefficient depends on:

- the length of the specimen: the greater the length the smaller is the ratio between the uncertainty in the measurement of length and its variation,
- the degree of precision with which the temperature of the specimen is measured, and
- the degree of precision with which the variation in the length of the specimen is measured.

## 2.2 MICROSCOPIC (LATTICE) MEASUREMENTS

The lattice constants of solids are usually determined using X-ray diffraction techniques with the help of Bragg's relation

$$n\lambda = 2d \sin \theta \quad (2.2.1)$$

where  $\lambda$  is the wavelength of the incident beam of X-rays and  $\theta$  is the glancing angle (Bragg angle) for a given reflection. In practice, only first-order reflections ( $n = 1$ ) are considered. The alteration in the distance between the atomic planes, or the lattice spacing,  $d$ , consequent to the expansion of the solid when the temperature is altered will be reflected as a change in the parameter  $\theta$ . From the Bragg law, we get

## Methods of Measurement of Thermal Expansion of Solids

### CHAPTER 2

#### 2.1. INTRODUCTION

Various methods of measurement of thermal expansion are discussed briefly here. The literature contains a wealth of information on apparatus for measuring thermal expansion. Though a review of the various techniques was given by Mezzetti (729) as well as by Verhaeghe *et al.* (1115), it will be useful to include them in the present volume. On the basis of the physical principle involved in the measurements, the different methods can be classified under two general headings: 1. *Microscopic* (lattice) expansion measurements, and 2. *Macroscopic* methods. The observations on thermal expansion can be made using either a *static* procedure or a *dynamic* procedure. In the static procedure the temperature of the material under investigation is maintained constant for a certain interval of time, and the variation of the length that takes place during the passage from one temperature to the other is measured successively.

The measurement is thus carried out between two different conditions of thermal equilibrium, and this leads to an accurate knowledge of the variation of length with temperature. On the other hand, in the dynamic procedure, the temperature of the specimen is varied continuously, and indirect observations on the variation of the length of the specimen are made simultaneously. This procedure is less cumbersome than the static method; however, the temperature in the interior of the specimen may not be uniform, and the results obtained thereby may not be very accurate unless the variation of temperature is maintained at a very low rate. The dynamic method thus adopted has the added advantage that observations can be made through phase transformations, if any, occurring in the specimen.

#### 2.1.1. Sensitivity

An examination of the Grüneisen formula (1.2.1) expressed as



$$\frac{\Delta d}{d} = \frac{\Delta \lambda}{\lambda} - \Delta \theta \cdot \cot \theta \quad (2.2.2)$$

For a closely constant spectral distribution  $\Delta \lambda \approx 0$ , and for large  $\theta$ , the shift in angle,  $\Delta \theta$ , becomes a sensitive measure of lattice expansion. Therefore equation (2.2.2) becomes

$$\frac{\Delta d}{d} = -\Delta \theta \cdot \cot \theta \quad (2.2.3)$$

These X-ray diffractometric methods fall under four groups:

- (1) The single crystal Bragg reflection method of Laue,
- (2) The powder-pattern (Debye-Scherrer) method,
- (3) Rotating (or oscillation) crystal method, and
- (4) Rotating-camera technique.

In all these methods the diffracted X-rays are recorded, generally, on a photographic film, and sometimes with the aid of ionization chamber or counters. The mounting of the film in an X-ray camera can be done in one of the three ways, namely, the *Van Arkel* (33), the *Bradley-Jay* (128) and the *Straumanis* or "asymmetric" (Levins & Straumanis) (485) methods. These are shown schematically in Fig. 2.1.

In the *Van Arkel* method, direct measurement of the angles of higher-order lines is obtained because the lines are all close together on the film. This is the case with the *Straumanis* method also. Both these methods require an inordinate length of film. On the other hand, in the *Bradley-Jay* method the higher-order angles are measured by the interposition of knife-edges, and it is necessary that the angle subtended by these knife-edges at the centre of the camera should be known (of course, after

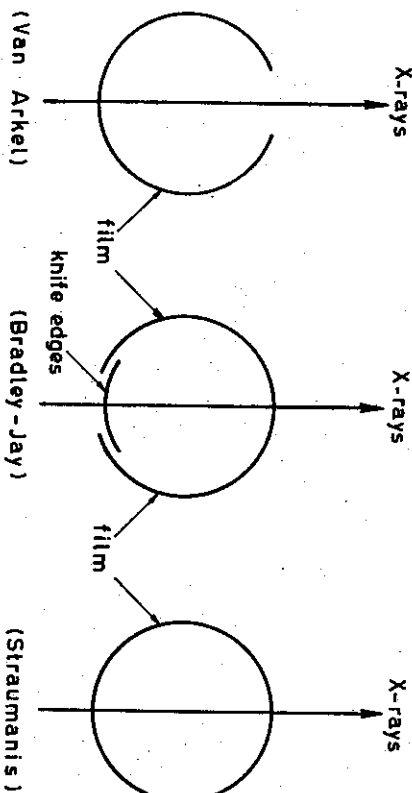


Figure 2.1.

centering the camera on the table of the spectrometer). This is somewhat a disadvantage, though the *Bradley-Jay* camera can easily be adapted to take two films of moderate length by introducing another set of knife-edges opposite to the first. An alternative to this is to measure the diameter of the camera and calculate the corresponding angle by knowing the distance between the knife-edges.

Irrespective of these variations in the techniques, all diffractometric dilatometers will have the specimen chambers (Cameras) modified in such a way as to permit the variation of specimen temperature and its measurement. The Debye-Scherrer technique is extensively used because it does not require the specimen in the form of a single crystal. Bond (118) has reported that with nearly perfect crystals the lattice constants can be measured to a few ppm. The highest precision appearing in the literature is that of *Straumanis & Aka* (1052), who report 0.00005% for a sample of high purity germanium. The accuracy in the measurement of angle  $\theta$  can be pushed up, in a diffractometer, by using non-photographic recording of different X-rays, like Geiger counter or scintillation counter along with rate meter and an automatic chart recorder. Here the Geiger counter could be moved over the graduated scale either by a spherometer or by a synchronous motor, and the readings of the counter positions could be read.

## 2.2.1. Advantages

The X-ray method has the following advantages over the other methods in dilatometry to be described later. They are:

- (i) It is an absolute method for determination of the value of  $\alpha$ , whereas most other methods make use of a reference standard at the temperature of the specimen.
- (ii) It determines the dimensions of the crystal unit cell, unaffected by the eventual impurity present in the crystal lattice. This is not so in the case of a macroscopic measurement. The knowledge of lattice thermal expansion is significant from the point of view of comparison with theory.
- (iii) The X-ray camera, in which the film is at room temperature throughout the investigation, is unaffected by errors arising indirectly from the effects of temperature gradients upon other parts of the apparatus.
- (iv) A small quantity of the specimen is sufficient to yield the required information. Therefore X-ray techniques are often the preferred method whenever the specimen is anisotropic because all the other methods require larger specimen size.
- (v) A single experiment yields complete information on the expansion coefficient along various directions in an anisotropic crystal.

(vi) The powder technique is suitable to study variation of  $\alpha$  with temperature through phase transitions, irrespective of the order of phase change.

(vii) The sensitivity of measurements in  $\frac{\Delta d}{d}$  of about  $4 \times 10^{-6}$  will be maintained down to temperature of  $\Theta_D/10$ .

One main disadvantage of the X-ray method is that dynamic measurements (continuous study of the variation of lattice spacing as the temperature of the specimen is varied continuously) are not possible, and this makes this method useless as a tool to judge the nature of the expansion anomaly in a phase change.

There are five categories of error which may be discerned in the determination of an accurate lattice constant by a Debye-Scherrer method:

(i) Subjective observational errors in the measurement of line positions on a film.

(ii) Random observational errors in the measurement of position of the diffraction line on a film.

(iii) Systematic errors inherent in the method (e.g., eccentricity of specimen mounting, absorption of X-rays by the specimen, specimen height). At  $\theta = 90^\circ$ , these errors in the determination of  $\theta$  are almost zero.

(iv) Systematic errors which do not vanish at  $\theta = 90^\circ$  (refraction, uncertainty in wavelength standards).

(v) When the results are extrapolated graphically to  $\theta = 90^\circ$  (when the errors in (iii) are almost zero), subjective errors arise.

These errors have been discussed by Bond (118). Some of these errors are eliminated by the type of mounting of the film in the camera and by other improved features of the camera.

An X-ray dilatometer essentially consists of an X-ray source and a precise low temperature or high temperature camera or an alternative arrangement to record the diffracted intensity. The X-ray camera should have the facility to vary the temperature of the specimen and to measure its value and to keep the specimen at any desired temperature. Several types of X-ray cameras have been developed to yield better results, and a few of them will be mentioned below.

### 2.2.2. Debye-Scherrer Method

(a) A modified powder camera was used by Figgins et al. (316) who adopted the Van Arkel type of mounting of film. The powdered specimen was in the form of a wire. The temperature of the specimen could be varied from 20°K to room temperature, and it could be maintained at any desired value within 0.04°K. With the same precision it could be

measured by a calibrated thermocouple. The reported sensitivity in the determination of  $\frac{\Delta d}{d}$  was  $5 \times 10^{-6}$ , approximately.

(b) A precision powder diffractometer for the measurement of thermal dilation has been used by Otte et al. (799). Ray (894) has reported an X-ray low-temperature camera suitable for thermal expansion study.

### 2.2.3. Rotating Crystal Method

In this method the specimen is in the form of a single crystal which must be mounted carefully so that its crystallographic axes are in some known direction in relation to the position of the film. In a rotation method the specimen is mounted at the centre of a cylindrical camera and the film is held in a vertical cylindrical arrangement and provision is made for rotating the crystal or for oscillating it through some small angle of  $5^\circ$  to  $10^\circ$ . A set of spots will be formed on the film corresponding to reflections from certain positions (of the crystal) where the Bragg condition will be satisfied. Analysis of a powder photograph is easier than that of either of the single crystal diffraction patterns. Straumanis (1050) has described the construction of a precision camera for rotating crystal as well as powder technique. Here the Straumanis type of mounting film in the camera is adopted. Only the back-reflection angle  $\varphi$  ( $= 90^\circ - \theta$ ) is measured, and a knowledge of camera radius is unnecessary. This way one avoids film thickness and shrinkage errors, because the precise reflection angles  $\varphi$  can be calculated from the films themselves at any time. Therefore neither a reference standard nor any calibration of the camera is required.

A rotating single-crystal back-reflection X-ray diffraction technique has been used in the range  $8^\circ$  to  $100^\circ$ K by Simmons & Balluffi (994). The estimated error in the determination of  $\alpha$  is reported to be  $1 \times 10^{-7}/^\circ$ K.

### 2.2.4. Rotating-camera Technique

A back-reflection "rotating-camera" technique, where a flat film is used, has been described by Batchelder & Simmons (79, 80) for determining lattice expansivity. In this method the camera is oscillated  $\pm 45^\circ$  of arc about appropriate settings on one side of the normal to the diffracting planes. The expansivity can be measured more accurately than the lattice constant itself because, by equation (2.2.3.) only the change in the position of the lines is measured. Here film shrinkage error and refraction error are present. A possible experimental error of  $\pm 16$ " in

$\theta$ , at  $78^\circ$  to  $85^\circ$ , arises principally from uncertainty in locating the peak of the diffraction maximum in the film. Batchelder et al. (77) used this technique for the study of neon single crystals in the temperature range  $2.5$  to  $23.9^\circ\text{K}$ . The unique advantage of this rotating-camera technique over the other methods is that not only the temperature but also an external hydrostatic pressure applied to the specimen can be varied. The reported accuracy is  $15$  ppm in lattice parameter and  $7$  ppm for relative expansion  $\Delta d/d$ . Reference may be made to the papers of these authors for more details regarding this method and the X-ray camera used.

### 2.2.5. Single Crystal Bragg Method

By a suitable choice of wavelength, a particular order of reflection can be obtained at a glancing angle of nearly a right angle, and recorded on a film in a back-reflection camera using Van Arkel method of film mounting. A small change in  $d$  is reflected as a large change in  $\theta$ , when  $\theta = \pi/2$ . For thermal expansion measurements this method was used by Megaw (713). In this technique a correction for the error due to shrinkage of film has to be made while calculating lattice constants. This error in the measurement of the position of the spot, if uniform, introduces only a negligible error in the value of  $\alpha$ . Bond (118) has described a good diffractometer method which, in principle, can be used for high-precision thermal expansion measurements.

In a very recent paper on thermal expansion using the powder technique, Sohan Singh et al. (1022) have used a new method of determining the lattice constant. In this method the back-reflection powder-patterns

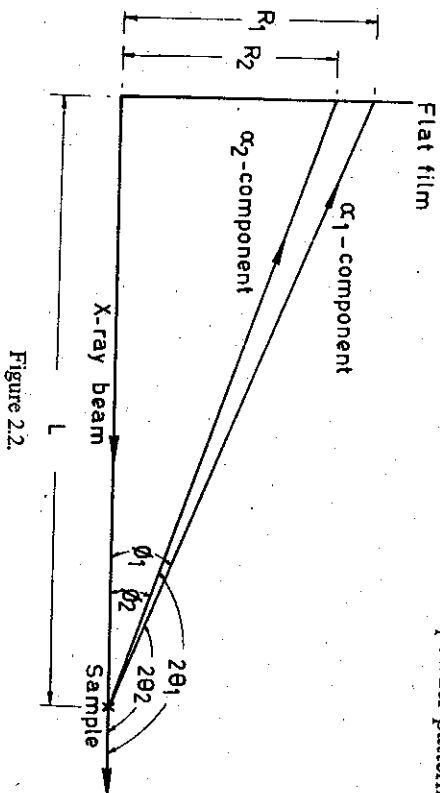


Figure 2.2.

*Methods of Measurement of Thermal Expansion of Solids* 13

were taken in a flat film using a  $\text{Cu K}_\alpha$  radiation. The back-reflection is shown schematically in Fig. 2.2.

The powder-pattern contains well-separated sharp rings of the components  $\alpha_1$  and  $\alpha_2$ . Using a comparator the diameters  $2R_1$  and  $2R_2$  of the reflection ( $hkl$ ) were measured to  $0.002$  mm. Average value of ten such measurements on a particular ring was used for the final calculations. Let  $\phi_1$  and  $\phi_2$  be the reflection angles of the radiations  $\alpha_1$  and  $\alpha_2$  corresponding to the wavelength  $\lambda_1$  and  $\lambda_2$ , respectively. Applying the relation

$$\frac{R}{L} = \tan \phi = \frac{\lambda \sqrt{4d^2 - \lambda^2}}{\lambda^2 - 2d^2} \quad (2.2.4)$$

to the two rings in the film, and eliminating  $L$ , film-to-crystal distance (which is not measurable), one gets

$$Ad^6 + Bd^4 + Cd^2 + D = 0 \quad (2.2.5)$$

where

$$A = 16(\lambda_2^2 R_1^2 - \lambda_1^2 R_2^2)$$

$$B = -4\{\lambda_2^2 R_1^2(4\lambda_1^2 + \lambda_2^2) - \lambda_1^2 R_2^2(4\lambda_2^2 + \lambda_1^2)\}$$

$$C = 4\lambda_1^2 \lambda_2^2 (\lambda_1^2 + \lambda_2^2)(R_1^2 - R_2^2)$$

$$D = -\lambda_1^4 \lambda_2^4 (R_1^2 - R_2^2)$$

Equation (2.2.5) eliminates the use of a standard specimen, and a solution of equation (2.2.5) yields the value of the unit cell dimension

$$a = \sqrt{h^2 + k^2 + l^2} \cdot d \quad (2.2.6)$$

It is reported that almost all the systematic errors are eliminated in this procedure because one of the rings functions as a standard and is close to the other ring; the value of  $d$  obtained thus will be correct to  $\pm 0.001$  Å.

### 2.2.6. Evaluation of the Value of $\alpha$ from X-ray Data

Depending upon the method of analysis of the lattice parameter versus temperature data, one gets either the true or the average value of the thermal expansion coefficient,  $\alpha$ . A brief discussion on this topic has been given in a review article by Deshpande & Mndholkar (246) from the available methods in the literature. Since they are found to be useful they will be discussed here. Firstly, the X-ray data is processed to obtain the value of  $\frac{da}{dt}$  at different temperatures. Then the zero-coefficient of thermal expansion can be calculated from the definition,

$$\alpha = \frac{1}{a_0} \frac{da}{dt} \quad (2.2.7)$$

where  $a_0$  is the value of the cell parameter at the zero degree of a temperature scale. The mean value of  $\frac{da}{dt}$  may be obtained by finding out the difference between the values of  $a$  at two neighbouring temperatures, and then the difference  $\Delta a$  is divided by the temperature difference  $\Delta t$  (Wilson, 1155). In a graphical method (Owen & Richards, 802; Deshpande & Mudholkar, 246; Dutta, 283; Nicklow & Young, 771) the lattice constants are plotted against the temperature,  $t$ , in a large graph sheet and the mean value of  $\frac{\Delta a}{\Delta t}$  were obtained from this graph; where  $\Delta t$  is usually a few tens of degrees. The average thermal expansion at that temperature is given by the relation

$$\alpha = \frac{1}{a_0} \cdot \frac{\Delta a}{\Delta t} \quad (2.2.8a)$$

Here the accuracy in  $\alpha$  is estimated to be about 5%. The same method can be applied to obtain the true value of  $\alpha$  by evaluating the slopes of the smooth curve at the desired temperatures.

$$\alpha_{true} = \frac{1}{a_1} \cdot \frac{\delta a}{\delta t} \quad (2.2.8b)$$

Thus the values of  $\alpha$  at every temperature corresponding to the slope are found. A least squares treatment of the  $\alpha - t$  data, thus determined, then gives the value of  $\alpha$  in an empirical form,

$$\alpha_t = A + Bt + Ct^2 \quad (2.2.9)$$

where  $A$ ,  $B$  and  $C$  are constants.

In a non-graphic method (Stokes & Wilson, 1047; Pathak & Pandya, 823, 824; Pathak *et al.*, 825; Kempter *et al.*, 536; Hall, 427; Hovi *et al.*, 468, 469, 470) the lattice parameter data were fitted by the method of least squares as a quadratic function of temperature,

$$a_t = a_0 + a_1 t + a_2 t^2 \quad (2.2.10)$$

where  $a_0$ ,  $a_1$  and  $a_2$  are constants.

By differentiating this parabolic equation we get

$$\alpha_t = \frac{1}{a_0} \cdot \frac{da}{dt}$$

$$\alpha_t = \frac{a_1}{a_0} + 2 \frac{a_2}{a_0} t \quad (2.2.11)$$

This method results always in a linear variation of  $\alpha$  with  $t$ , which is naturally incorrect. An improved variation of this method is to fit the  $a - t$  data with a polynomial of degree three in  $t$ ,

$$a_t = b_0 + b_1 t + b_2 t^2 + b_3 t^3 \quad (2.2.12)$$

where  $b_0$ ,  $b_1$ ,  $b_2$  and  $b_3$  are constants.

Such a procedure was adopted by Owen & Williams (808), Dheer & Surange (265, 266), Dutta (284) and Singh (997). This latter procedure is more cumbersome and requires the aid of a computer, and so it is rarely followed. Even this method has been extended to fit a polynomial of degree four in  $t$  (Dutta & Dayal, 287). Introducing a new term, percentage expansion, defined as  $\left( \frac{a_t - a_0}{a_0} \right) \times 100$ , Lang (607) expressed:

$$\frac{\Delta a}{a} (\%) = at + b't^2 + c't^3 \quad (2.2.13)$$

where  $a'$ ,  $b'$  and  $c'$  are constants.

## 2.3. MACROSCOPIC METHODS

In this category there are various techniques developed at different laboratories:

- (1) Comparator method,
- (2) Mirror and Optical lever method,
- (3) Two-terminal capacitance method,
- (4) Three-terminal capacitance method,
- (5) Variable-transformer (or differential transformer) technique,
- (6) Optical interferometric techniques,
- (7) Dilatometer with grids,
- (8) Methods other than those listed above, and
- (9) Automatic recording of dilatation.

The various methods cited above have different degrees of sensitivity; techniques using the optical lever, three-terminal capacitance and the variable transformer possess very high sensitivity so that these cannot be used at their full sensitivity at room temperatures. Thus these high sensitivity techniques have little advantage in terms of sensitivity over the two-terminal capacitance and interferometric methods, except at very low temperatures.

### 2.3.1. Comparator Method (Conway & Losekamp, 199)

In this method the specimen should be long and its change in length is measured by means of a comparator or a similar device. This method is not in practice for the study of thermal expansion of crystals because long specimens are very difficult to obtain. Its usual precision is reported to be about  $10^{-4}$  cm. only.

### 2.3.2. Methods Incorporating an Optic Lever

In this technique the dilatation of the specimen is converted, by means of an optical lever, into a light signal. The dilatation of the specimen causes a tilt of a mirror or optical lever arrangement, and the incident beam of light will be reflected according to laws of reflection (Chevenard, 1975). Later workers mounted the specimen in the form of a rod in a thermostat in such a way that it transmits its elongation, through a rod of low coefficient of dilatation (however, known), to the mechanical assembly which causes the rotation of the mirror. Finally the reflected light from the mirror is observed visually with the aid of optical instruments. In another type, the sample under examination produces directly the rotation of the mirror. This technique employs built-in micro-optic auto-collimators and a kinematically designed twin-strip mechanism and an optical system (Huzan et al., 481). The twin-strip mechanism (otherwise known as Ayrton strip) contains a flat strip whose centre is twisted to elastically permanent set. In this condition if this flat strip is held fixed at its ends, subsequent elastic displacement of the ends will result in an untwisting. If  $\Theta$  is the total angular twist from one end to the centre of a strip of total length  $L$ , width  $2a$ , and thickness  $2b$ , with  $b \ll a$ , it can be shown that the rate of change of  $\Theta$  with respect to  $L$  is given by Shapiro et al. (967) as follows:—

$$-\frac{d\Theta}{dL} = \frac{\Theta/L}{\frac{4n}{Y}\left(\frac{b}{a}\right)^2 + \frac{12}{5}\left(\frac{a\Theta}{L}\right)^2} \left\{ 1 + \left(\frac{a\Theta}{L}\right)^2 \right\} \quad (2.3.1.)$$

where  $Y$  is Young's modulus and  $n$  is rigidity modulus of the material of the strip.

Thus a maximum sensitivity is given by

$$-\frac{d\Theta}{dL} \Big|_{\text{optimum}} = + \frac{1}{8b} \sqrt{\frac{5Y}{3n}} \dots \quad (2.3.2.)$$

This formula was tested and found to be correct. The material for the

strips should be soft enough to twist permanently and stiff enough as not to yield under a tensile load. The material used for the strip was a precipitation hardened alloy, Cu + 1.9% Be. The strip was hardened by the precipitation of a second phase by heating it to 300°C for one hour with its ends clamped. Such a strip of 0.55 mm by 0.035 mm, twisted to the optimum pitch of about 2 radians/cm, had a sensitivity of about 165 radians/cm. The dilatometer used by Shapiro et al. (967) is illustrated in Fig. 2.3, while Fig. 2.4 shows their optical lever system. The optical lever system is similar to the one developed by Jones (514).

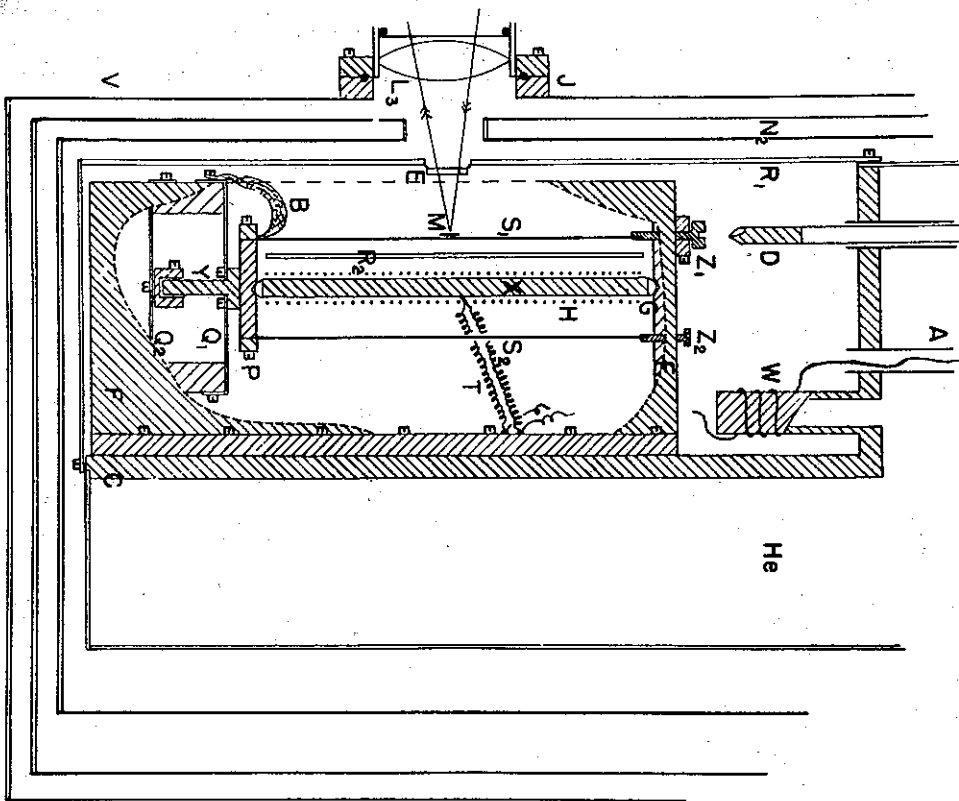


Figure 2.3. (Schematic view of the dilatometer)

### Thermal Expansion of Crystals

X	: rod-like specimen
F	: Frame
P	: Platform
G	: Quartz hemispheres
H	: 50 B & S manganin wire of 500Ω serving as heater
T	: Thermocouple (Au + 2.1% Co versus Ag + 0.37% Au)
S <sub>1</sub> , S <sub>2</sub>	: Two Ayrton strips
M	: Mirror
L <sub>3</sub>	: Front lens of the optic lever
Z <sub>2</sub>	: screws
Z <sub>1</sub>	: rod and collar
D, Y	: rods
Q <sub>1</sub> , Q <sub>2</sub>	: Be - Cu strip springs
B	: soft copper braid
C	: ¼ in. copper side wall
He	: liquid helium bottle
A	: Pumping line
W	: threaded copper-well
R <sub>1</sub> , R <sub>2</sub>	: Copper radiation shields
E	: heat absorbing glass (Corning CS - 69)
V	: Triple-walled vessel of monel
N <sub>2</sub>	: liquid air container
J	: Flange

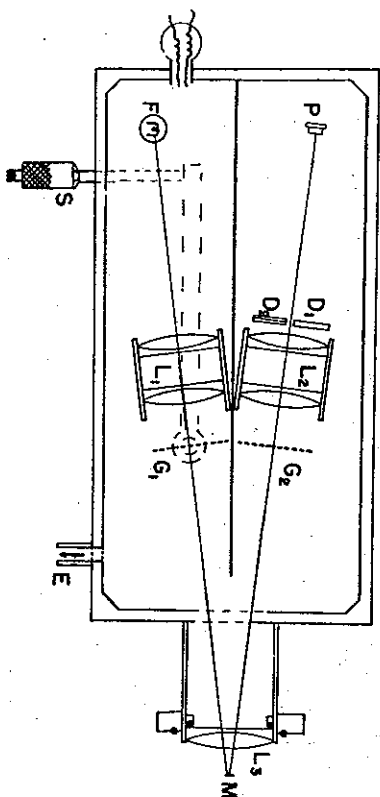


Figure 2.4. (Optic Lever)

L <sub>1</sub> , L <sub>2</sub> , L <sub>3</sub>	: Coated achromatic doublet lenses of 18 cm. focal length
F	: lamp filament
M	: Mirror
P	: split-photocell
G <sub>1</sub>	: grid
G <sub>2</sub>	: split replica
D <sub>1</sub> , D <sub>2</sub>	: periscope prisms
S	: Micrometer and lever arrangement
E	: tube for evacuation

### Methods of Measurement of Thermal Expansion of Solids 19

At present, the limit of detection of this dilatometer, employing specimens about 10 cm long, is about 0.03 Å change in length. An improved version of this method has been described by Pereira et al. (1601, 1602).

#### 2.3.3. Two-Terminal Capacitance Technique

In the capacitance dilatometer the specimen dilates, and this alters the distance between the plates of the condenser producing variations in capacity. The dilatometric condenser in series with a standard capacitor forms part of a Colpitt's circuit oscillating at a radio frequency. Thus the change in resonance frequency,  $f_r$ , of this oscillator can be detected by the heterodyne beat method and can be compensated for by altering the capacity of the standard condenser  $C_0$ . The capacity  $\delta C$  needed for compensation is a direct measure of the expansion or contraction of the specimen. Bijl & Pullan (101) were the first to use this technique, followed subsequently by Dheer & Surange (266) and Madaiah & Graham (664). Resonance frequency is given by

$$f_r^2 = \frac{1}{4\pi^2 L(C + E)} \quad (2.3.3)$$

$$2 \frac{\delta f_r}{f_r} = - \frac{(\delta C + \delta E)}{(C + E)}$$

where  $C$ ,  $E$  and  $L$  are, respectively, the dilatometer capacity, distributed capacity and inductance of the tank coil, and  $\delta E = 0$ . The dilatometer is schematically shown in Fig. 2.5, (Bijl & Pullan, 101).

In this dilatometer, the specimen  $S$  is cylindrical in shape with a length of  $\sim 2$  cm. It is held stably on an optically flat fused quartz plate  $Q$  resting on a quartz ring  $q$ . The specimen is surrounded by a hollow copper cylinder  $R$  of slightly smaller length than  $S$ . This serves as a reference standard in the dilatometer, and any measurement, will, therefore, yield values relative to that of  $R$ .  $R$  is fixed in position by means of steel springs  $S_1$  attached to the base plate  $P$ . The upper end of the specimen is rounded and supports a copper plate  $P$ , which can be moved up or down to the extent of  $\sim 0.5$  mm. To allow for this free motion of the plate  $P$ , it is attached to two phosphor bronze membranes  $M_1$  and  $M_2$ . The capacity between  $P$  and  $R$ , separated by a small gap of  $\sim 0.4$  mm, depends only on the difference in lengths between the specimen  $S$  and the ring  $R$ .

This assembly with other features (not to be described here) is built in a vacuum tight jacket which is also surrounded by another similar jacket leaving an annular space in between them. The temperature of inner jacket, and hence the specimen, can be varied from 20°K to 300°K

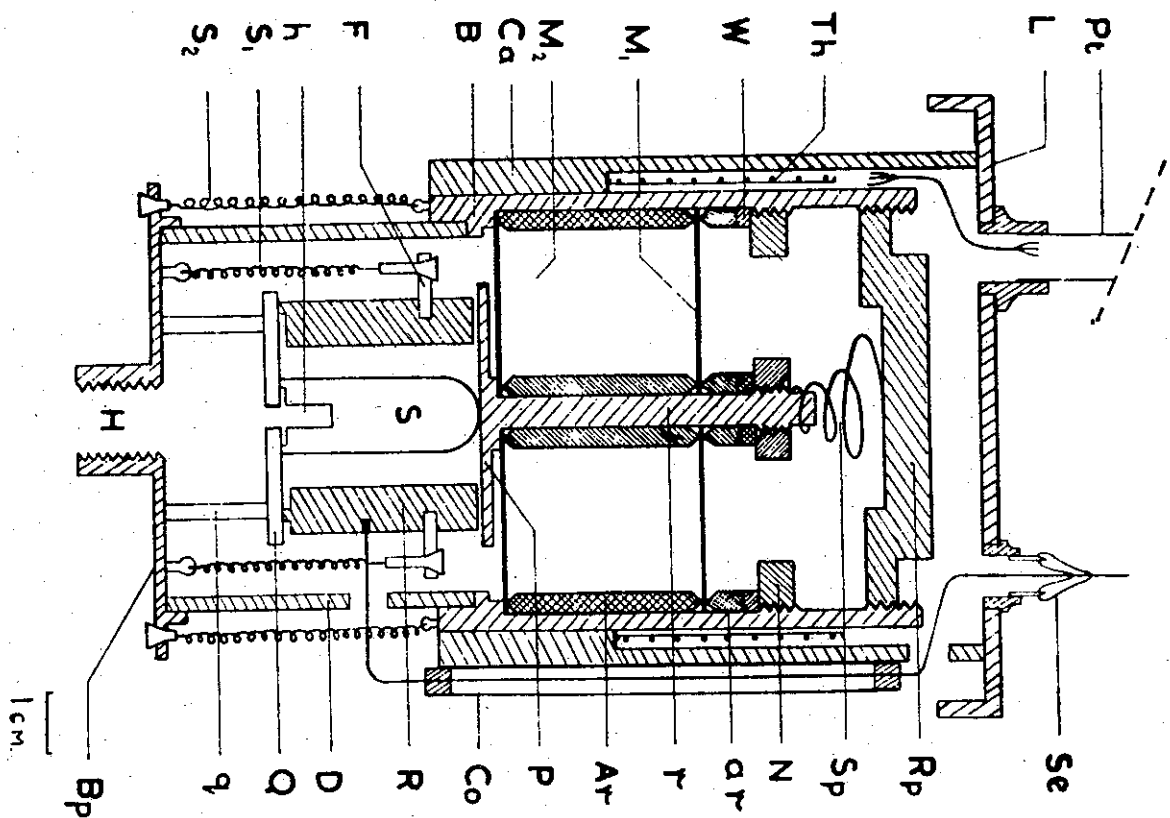


Figure 2.5.

by means of a heating element of the inner jacket. In operation the whole assembly is immersed in a refrigerant.

The dilatometric condenser in series with a standard capacitor forms part of a Colpitt's circuit oscillating at radiofrequencies. The wavemeter having an accuracy of 20 ppm will give a precision of  $2 \times 10^{-5}$  in the determination of  $\delta l/l$ . Taking  $(C + E) \approx 50$  pF it is found that the measurable variation is  $\delta C \approx 1.8 \times 10^{-3}$  pF or  $\delta C/C \approx 4 \times 10^{-5} \approx \delta l/l$ , where  $l$  is the separation between the plate (P) and reference ring R. Taking  $l \approx 0.2$  mm,  $\delta l \approx 8 \times 10^{-7}$  cm. This change  $\delta l$  is produced by the change in length of the specimen  $L \approx 2$  cm.

$$\therefore \delta l/L = 4 \times 10^{-7}$$

This accuracy can be pushed up by better design features of the dilatometer.

### 2.3.4. Three-Terminal Capacitance (3T - C) Technique

As mentioned earlier measurements of  $\alpha$  values at temperatures below  $(\Theta_D/50)$  involve detection of movements as small as  $10^{-9}$  cm. or less.

- Figure 2.5. (Two-terminal capacitance dilatometric cell)
- S : Specimen (about 2 cm. length)
  - Q : fused quartz optically flat plate
  - q : Quartz ring
  - R : Copper reference ring (one plate of the Capacitor)
  - P : Copper plate forming the capacity between R
  - Co : Co-axial line
  - Se : Copper-glass seal
  - h : a central hole in S
  - F : Fibre disc
  - S<sub>1</sub> : steel springs
  - Bp : base plate
  - I : vertical rod
  - M<sub>1</sub>, M<sub>2</sub> : two carefully annealed phosphor bronze membranes
  - B : Barrel
  - Ar, ar : knife-edged annular rings
  - W : washer
  - N : locking nut
  - Sp : Phosphor bronze conical spring
  - Rp : a plate
  - Ca : vertical case
  - L : lid
  - Th : Platinum resistance thermometer
  - Pt : Pumping tube
  - D : annular ring
  - H : threaded boss

One of the methods is the three-terminal capacitance technique developed by White (1138, 1139). Such a dilatometer described recently by Carr et al. (163) has a sensitivity of  $\sim 10^{-10}$  cm, and measurements of  $\alpha$  are possible with an error of  $\sim 10^{-10}/^\circ\text{K}$ . This means  $\alpha$  may be measured as precisely as the specific heat  $C_p$ , or, the elastic moduli  $c_{ij}$ , so as to enable calculation of  $\gamma$  for making comparison with the theoretical predictions of anharmonic models (Barron & Batana, 67).

#### (a) Principle

This method essentially consists of accurate comparison of small capacitances at different temperatures by means of an a.c. bridge. In a series of papers White (1138, 1139, 1141, 1146, 1147, 1151) has described this technique and its development while measuring thermal expansion of several solids. A three-terminal capacitor (1139) is illustrated in Fig. 2.6, in which 1, 2, and 3 are conducting surfaces. The conducting surface (3) surrounds completely the other two electrodes, and in practice forms the local earth shield.  $C_{12}$  defines then the direct capacitance between the surfaces (1) and (2).

Two such capacitances may then be connected in a transformer bridge (Fig. 2.7), in such a way that the ground capacitances  $C_{13}$  &  $C_{23}$  only shunt the ratio arms of the transformer and the detector D. Though this eliminates  $C_{13}$  and  $C_{23}$  in the balance equilibrium, yet the sensitivity

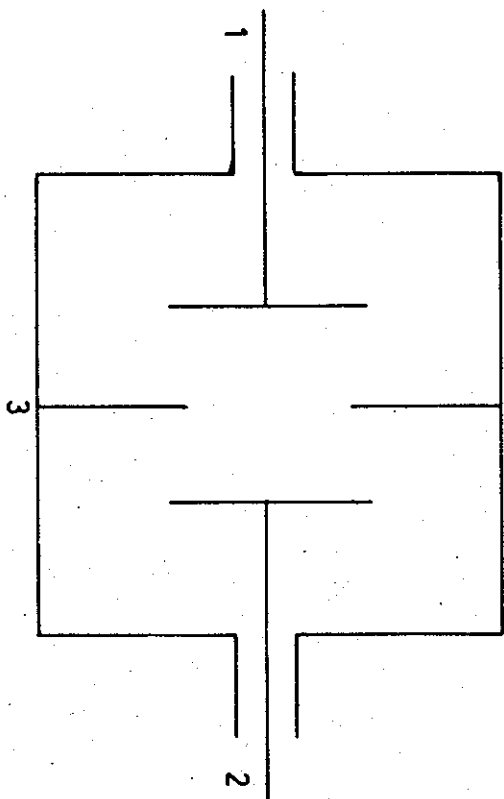


Figure 2.6.

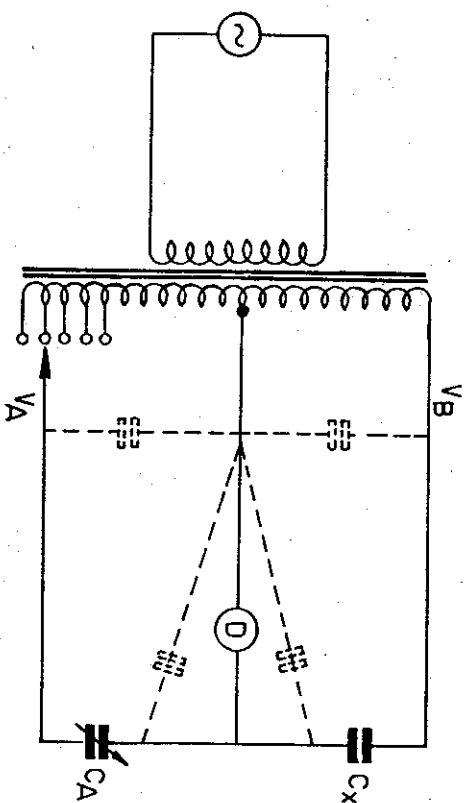


Figure 2.7.

of the bridge depends on them. Under proper conditions  $\frac{C_A}{C_x} = \frac{V_B}{V_A}$ , where  $V$  represents the voltage appearing on the relevant terminal of the transformer. Either the transformer arm or capacitance arm or both may function as the variable arm (or arms) of the bridge. The block diagram of the transformer bridge is shown in Fig. 2.8. The chief components of this bridge are a power amplifier, a ratio-transformer, a capacitance

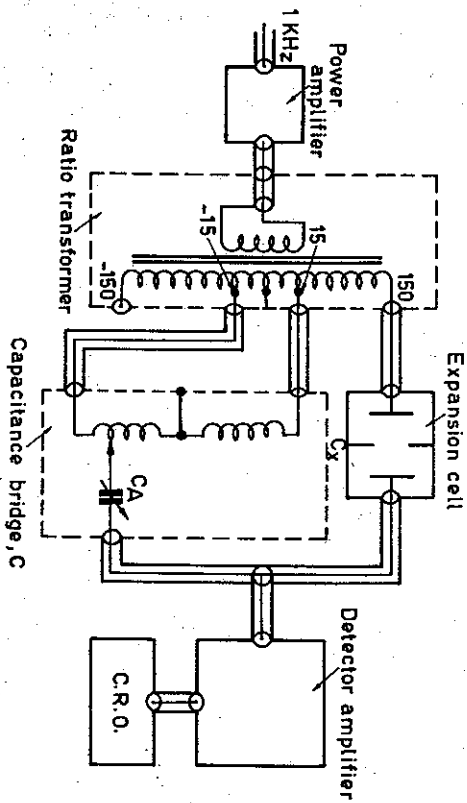


Figure 2.8.



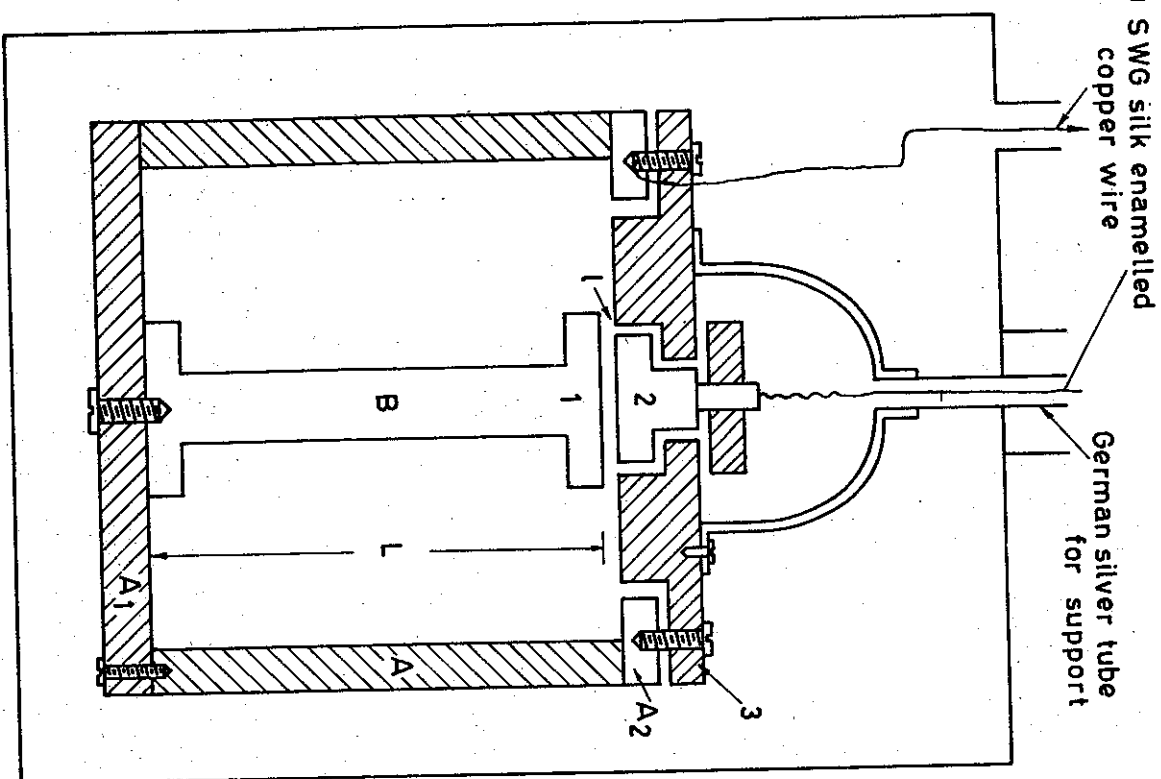


Figure 2.9.

bridge and detector system. The power amplifier boosts the input 1 kHz supply to an output required to supply the bridge.

#### (b) Ratio-transformer

In this unit the tightly coupled sections of the secondary winding form two arms of the bridge. The electrically screened ratio-transformer has the secondary as  $(+150) - (+15) - (-15) - (-150)V$ . Carr et al. (163, 165) have given the details of the transformer and the bridge of good resolution and stability.

#### (c) Capacitance Bridge

The capacitor  $C_A$  in Fig. 2.8 is itself a bridge (not shown in the diagram). It may be 0 to 111.11110 pF in steps of  $10^{-5}$  pF. Its range can be extended by coupling to an available ratio-transformer so that ten times larger voltage may be applied to the unknown capacitor  $C_x$  than is applied to  $C_A$ . Seven fixed capacitors ranging through 0.0001, 0.001, ..., 10,100 pF and a tapped inductance form part of the bridge. These capacitors require high stability and therefore are sealed invar capacitors (design features of which are given by White (1141) and Carr et al. (165)).

#### (d) Detector System

The detector system consists essentially of a tuned amplifier and a bridge indicator in which separate indications of the conductance balance and capacitive balance are conveniently displayed on a CRO. The conductance balance implies that the current from one capacitor to the detector is identical both in magnitude and in phase with that from the other capacitor to the detector. The relatively large ground capacitances, of hundreds of pF, present in the leads to the expansion cell reduces the sensitivity of the detector. By including a tuning loop in the detector system, Carr et al. (163, 165) have achieved a resolution of about  $2 \times 10^{-7}$  pF.

#### (e) Dilatometric Cell (or Expansion Cell)

White (1139, 1141) has designed and perfected two cryostats, one for measurement of absolute values of and the other for relative measurement. These cells have a capacitance of about 5 to 20 pF each.

The expansion cell for relative measurements, otherwise called the "differential cell", is made completely from OFHC copper (plus brass

screws and mica washers). It is schematically shown in Fig. 2.9. It is a cylinder A of about 6 cm. long and 5 cm. diameter; in it is mounted the specimen B in bobbin shape (so as to reduce the mass of the material to be cooled or heated during a measurement). The end faces of the specimen are ground and lapped to a length,  $L$ , of 5 cm. (the degree of flatness being a few ppm of a cm.). The central electrode (2), the guard ring (3) and the support ring  $A_2$  have been assembled together with insulating washers (or a hot setting Araldite) into a unit whose down face has also been ground and lapped to a flatness of the same degree as the faces of B. The capacitance faces (1) and (2) have diameters of about 2 cm. and 1.27 cm, respectively. The gap,  $l$ , between (1) and (2) which forms the capacitance  $C_{12}$  is about 0.0254 cm. at room temperature. Separation between the cylindrical surfaces of (2) and (3) forming the annular gap is also 0.0254 cm. The lower lapped end of specimen is held firmly on to the lapped surface of  $A_1$  with a 4 BA screw and spring washer. To change specimens it is necessary to remove only three screws which attach  $A_1$  to the lapped face of A. Guard ring (3) is earthed through the metallic portion of the cryostat. The cryostat, which has otherwise conventional features, can be used for varying the temperature of the cell from liquid Helium temperatures to 300°K. When the temperature of the cell is altered, not only both the materials A and B dilate, but also all the components change their dimensions. Thus the relative variation in the lengths of the specimen and copper cell alters the 0.025 cm. gap and hence the capacitance  $C_{12}$ . White carried out measurements on a specimen of beryllium at different temperatures with respect to the dimensions of the outer cell. (Be was chosen because it has the  $\Theta_D \approx 1000^\circ\text{K}$ ; its value of  $\alpha$  is small at very low temperatures with respect to that of other materials under study and it can be calculated with sufficient degree of accuracy by using the Grüneisen relation.) Thus the dilatations of the sample relative to beryllium are obtained.

In the differential cell the expansivity of A should be known well in order to determine the relative expansion of specimen B. Therefore White (1139, 1141) designed an "absolute cell", primarily to know the expansivity of OFHC copper. This cell is schematically shown in Fig. 2.10. The copper cylinder (1) of 3.74 cm. diameter has well-polished cylindrical surface which forms one surface of the capacitor  $C_{12}$ . The outer cylinder (2) has a width of 1.5875 cm. and thickness of 0.3 cm, approximately. The annular cylindrical gap between surfaces (1) and (2) is of width 0.0254 cm. The inner cylinder is centrally supported by glass balls (0.3 cm. in diameter, ground and polished to be not more than  $\sim 10^{-5}$  cm. out of round) one each at either end. A change in  $C_{12}$  can be measured as a result of free radial expansion of the inner cylinder. D is a flexible

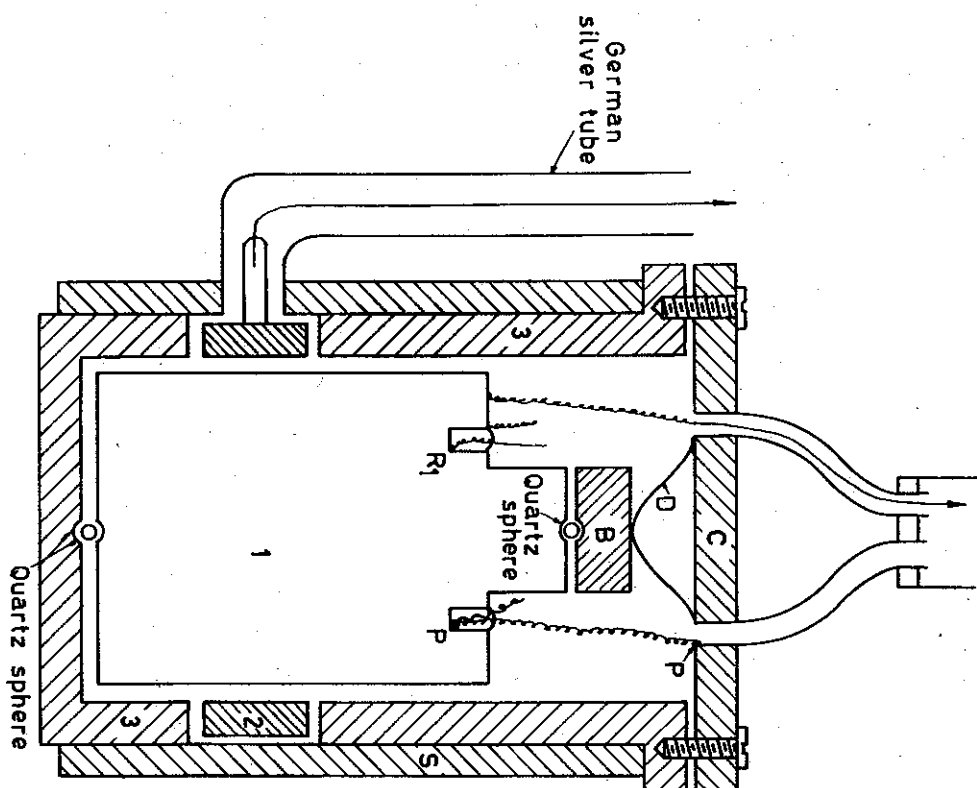


Figure 2.10.

diaphragm fixed to the top plate C along its circumference, and the copper block B is soldered to it at the centre. A thin layer of Araldite cement, of about 0.0254 cm. thick, separates the electrode (2) from both the sleeve cylinder S and the electrode (3). The cell is heated by the carbon heater ( $R_1$ ) of  $\sim 200 \Omega$  resistance. To measure the temperature a thermocouple (gold + 2.1% (at.) cobalt versus copper) is anchored at point P. The top plate C is attached to the flange of (3) through a polythene gasket ( $\sim 0.013$  cm. thick), by means of twelve 8BA brass screws. Until the

lowest temperature is reached with liquid He, helium gas surrounds the cylinder (1) and afterwards the gas is pumped out.

### (f) Calculation of Results

(i) *Differential Cell:* For a parallel-plate condenser, the relation

$$C = \frac{\pi r^2}{l} + \frac{\pi r w}{l + 0.22w} \left(1 + \frac{w}{2r}\right) \quad (2.3.4)$$

gives the capacity after including the correction term for distortion of the electric field near the edge of the plate.

where  $w$ : width of the gap between the electrode and guard ring;

$r$ : radius of the electrode (2); and

$l$ : the separation of electrodes (1) and (2).

For the cell described here,

$$2r = 1.27 \text{ cm,}$$

$$w = 0.0254 \text{ cm,}$$

$$\text{and } l = 0.0200 \text{ cm. (say),}$$

then  $C = 5.778468 \text{ pF,}$

$$\text{and } \frac{\Delta C}{\Delta l} \approx 2.86 \times 10^{-6} \text{ pF/\AA.}$$

(ii) *Absolute cell:* Capacitance of a coaxial condenser (of radii  $a_1$  and  $a_2$  with  $a_1 < a_2$ ) after applying correction for distortion of electric field near the end is given by

$$C = L \left\{ 2 \ln(a_2/a_1) \right\}^{-1} \left\{ 1 + \frac{wl}{L(l + 0.22w)} \right\} \quad (\text{in e.s. units}) \quad (2.3.5)$$

where  $l = a_2 - a_1$ ;  $L$  is length of the shorter cylinder (2). For the cell described here,

$$w = 0.0254 \text{ cm, } L \approx 1.5875 \text{ cm,}$$

$$a_2 \approx 1.8948 \text{ cm, } a_1 \approx 1.8694 \text{ cm.}$$

choosing  $l \approx 0.275 \text{ cm}$ , and  $(a_2 - a_1) \ll (a_2 + a_1)$ ,  $C \approx 61.20203 \text{ pF.}$

It is found that any small eccentricities in the coaxiality of the cell do not affect the capacity of the cell evaluation as before.

The principal random errors that affect the results arise from:

- (1) bridge sensitivity due to reference capacitor being not very stable and to the limited sensitivity of the detector, and

- (2) instability in expansion cells which arise by virtue of their method of construction.

With the aid of improved amplifier and detectors, more stable reference capacitors, smaller gaps and higher voltage, detection sensitivity of better than  $\sim 10^{-9}$  cm. has been reached (Philipp et al., 843).

In order to increase the sensitivity of measurements a remarkable technique has been employed in a differential cell by Telford & Swenson (1753). The capacitance cell described earlier is inverted such that the capacitor gap decreases as the temperature of the specimen is lowered. This results in maximum sensitivity in dilatation at low temperatures. This "inverted differential cell" has been used by Schouten & Swenson (1679) for precise measurements on potassium metal down to 2°K. The precision reported is better than 0.1% above 4°K, except below 4°K.

The study of thermal expansion of solidified gases below 10°K is carried out generally by the dilatometers used by Telford & Swenson (1753), Heberlein & Adams (1407), or by Veith, Coufal, Korpium & Lüscher (1776). But in these three dilatometric cells, the solidified gas grown elsewhere has to be transferred for mounting in the cell, or else the quality of the specimen cannot be controlled if it is grown in the cell. Tolkaev, Aleksandrovskii & Kuchnev (1759) have recently developed a dilatometric cell in which the gas can be solidified and grown within the cell. Parahydrogen was studied by them in the range 2° – 25°K.

### (g) Advantages and Disadvantages

Advantages of the 3 T-Capacitor technique are:

(i) This technique has a sensitivity of at least 0.05 Å at liquid helium temperatures; and it can be used to measure  $\alpha$  with an error of only  $\sim 10^{-10}/^\circ\text{K}$ . (0.1% precision has been reported below 2°K in an "inverted cell").

(ii) Relative or absolute measurements are possible by choosing the appropriate cell.

(iii) The reproducibility of the results show that the errors present in the measurement are only systematic.

Disadvantages are:

(i) It requires large specimen size and precise shaping of the specimen. Therefore this method cannot be used for most of the solids.

(ii) The sensitivity of  $\sim 0.05 \text{ Å}$ , is highly useful at temperatures below  $\Theta_D/50$ . However, this technique cannot be used for measurements of  $\alpha$  at higher temperatures with the same sensitivity.

(iii) Designs of the expansion cells are such that their fabrication is not easy.

After the introduction of this technique by White several metals and alkali halides have been studied at very low temperatures. White (1139, 1140, 1142, 1143, 1144, 1145, 1149, 1150, 1151, 1152, 11794-1802), Carr et al. (163, 164, 165), McCammon & White (703), Philip et al. (843), Donaldson & Lanchester (273), Andres (19), Schouten & Swenson (1679), Ott (1582) obtained data on praseodymium.

The "inverted differential cell" has been used by Schouten & Swenson (1679) for precise measurements (0.1%) on potassium metal at low temperatures down to 2°K. This provides additional data for the  $T = 0$  molar volume of potassium. The van Alphen-de Haas measurements on potassium could be interpreted based on this quantity.

### 2.3.5. Differential Transformer Method (Variable-Transformer Technique)

A perusal of the technique described earlier will reveal that those dilatometers differ from one another basically in the sensing device to detect change in dimensions. Robbins et al. (904) used the principle of a differential transformer as the sensing device in their dilatometry. In order to study the anharmonic character of lattice binding forces, and, in the case of metals, to isolate the electronic contribution from the lattice part of  $\alpha$ , which is important at temperatures below  $\Theta_D/50$ , Carr & Swenson (165) developed the earlier method to yield high sensitivity in detection of small changes of length. McLean et al. (1529) studied copper, silver and gold, whereas Case & Swenson (1274) measured  $\alpha$  of NaCl down to 1°K.

#### (a) Principle

The expansion sensing unit is an air-core transformer in which the astatic secondary can be moved relative to the fixed primary coil. There are two halves of the secondary coil (inner coil) such that their windings are in opposite directions (differential winding). When the secondary (of turns density  $n_2$ ) is centred within the primary (of turns density  $n_1$ ), there is no flux linkage between the primary and secondary coils on passing an alternating current; in other words, their mutual inductance is zero. While  $n_2 x$  turns, wound in one direction in the secondary, enter the central field region as a result of itself being displaced through a length  $x$ , an equal number of opposing turns leave. Since the secondary is wound symmetrically with its ends in a zero (or uniform) field, the net mutual inductance change for this motion is  $2\mu n_1 n_2 A_2 x$ , where  $A_2$

refers to the cross section of the secondary coil and  $\mu$  is the permeability of free space. For small motions ( $|x| \approx 1$  mm.) about a null position the coupling between the primary and secondary (as measured with a mutual inductance bridge) is a linear function of the displacement of the secondary coil. Carr & Swenson claim a mutual inductance sensitivity of 0.32 H/cm, or  $3.2 \times 10^{-3}$  micro-H/Å. The mutual inductance bridge can detect changes in mutual inductance of as small as one millimicrohenry which corresponds to a displacement of  $\frac{1}{3}$  Å, and this sensitivity is comparable with or better than that obtainable with other precise dilatometer techniques. Before describing more details on the design features of the dilatometer let us look into the advantages and disadvantages of this method.

#### Advantages:

- (1) A sensitivity of better than  $2 \times 10^{-10}$  cm. ( $\pm 0.02$  Å) can be realized for a 10 cm.-long sample in this technique so that measurements on thermal expansion can be performed down to liquid helium temperatures. This means a relative precision of 0.1% for  $\alpha \approx 3 \times 10^{-6}/^\circ\text{K}$ . The absolute accuracy is limited by the calibration and is estimated to be within 0.5% and 1% (Case et al. 1274).
- (2) It is an absolute method, as will be understood later, because no reference standard is involved in the dilatometer.

#### Disadvantages:

- (1) Large specimen size is one of the prerequisites for the study on a solid with this method. Therefore only a few substances can be studied using this dilatometer.
  - (2) It is very difficult to make measurements on even slightly magnetic or superconducting materials. This arises out of the serious difficulties due to the effects of even small iron concentrations near the variable-transformer.
  - (3) This dilatometer cannot be used with its full sensitivity for study at higher temperatures when the specimen length changes enormously.
  - (4) The design features of the expansion cell call for great skill so that it cannot be easily fabricated in all the laboratories.
- This dilatometer consists essentially of two main parts:
- (i) The expansion chamber which includes the specimen and the variable-transformer.
  - (ii) A mutual-inductance bridge and detector system.

(b) *The Expansion Cell*

An improved version of the expansion cell due to Sparks & Swenson (1024) is shown schematically in Fig. 2.11. The specimen is machined strainfree in the form of a rod of about 10 cm. long and 5 ~ 8 mm. diameter. The secondary of the variable-transformer is connected mechanically to the sample (enclosed in an evacuated chamber with a flexible window) by means of a thin fused quartz spacer (2 cm. long). In the figure the secondary support, which allows only longitudinal motion, is not shown. A heater of 40 ohms resistance is wound non-inductively over the sample

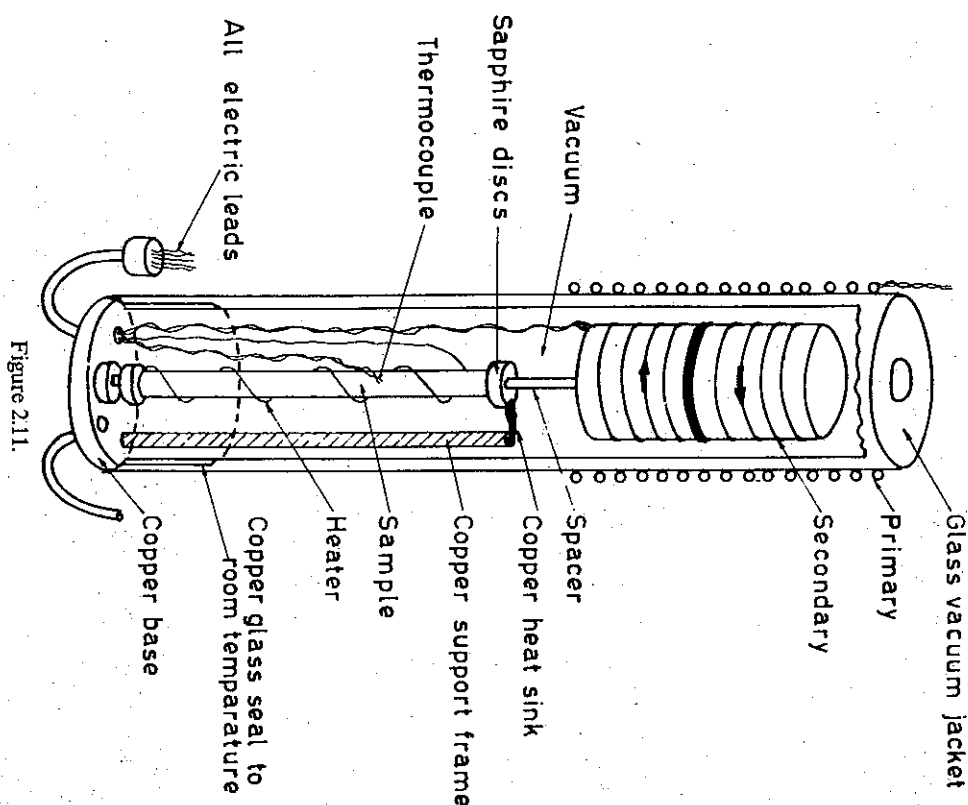


Figure 2.11.

and it is fixed to it by means of G.E. 7031 varnish. (A power of 35 mW supplied to the heater was found to raise the temperature of the sample to 25°K. from liquid helium temperatures). Spotlessly clean surfaces of a sapphire disc were used to function as thermal "breaks" to limit the flow of heat through this end of the sample. Such a sapphire disc makes use of the relatively high thermal impedance existing between two smooth, hard surfaces in a vacuum. Sapphire discs are glued to each end of the sample and also to heat sinks at the upper and lower portion of the sample chamber. The two discs at the bottom of the sample chamber are indented, and between them is placed a sapphire ball to act as a gimball bearing. Three horizontal nylon strings, spring-loaded to maintain tension and anchored to the frame of the chamber, allow only longitudinal motion of the sample. The upper heat sink is a copper foil directly anchored to a copper rod which terminates in a liquid helium bath.

Both the quartz spacer and the secondary of the variable-transformer are thermally anchored directly to the refrigerant by means of fine copper wires attached to copper posts. To prevent heating of the secondary due to eddy currents generated by the primary field, copper strips are inserted between the secondary windings and the system is anchored to the liquid helium bath in the same manner described previously. Still, when the cryostat was in operation, reports show that the secondary attained a temperature of 2 to 30 degrees above that of the refrigerant. But this is found to be not important so far as this difference in temperature is independent of the power input to the sample heater.

The variable-transformer is an air-core device consisting of independent primary and secondary coils. A typical variable-transformer, used by Sparks & Swenson, had its secondary formed of two halves (each 4.06 cm. long, and 2.54 cm. outer diameter) wound in opposite directions having 5000 turns each of No. 38 copper wire. These two halves are free standing (that is, no core material is involved) and bonded together using GE 7031 varnish. The coil had a resistance of 21 ohms and an inductance of 400 mH at 4°K. The fused quartz spacer is fixed at the geometrical centre of the coil. To allow only longitudinal motion, this coil is suspended from a glass-impregnated phenolic frame by six nylon strings (three on each end). The primary coil is wound on glass-impregnated phenolic hollow frame of external diameter 4.57 cm. For rough adjustment it can be slid on the glass vacuum jacket and finally it can be fixed in place. The primary has a centre portion and two equivalent end sections. The centre portion, 3.8 cm. long, has 2,500 turns of No. 38 copper wire wound in a clockwise direction. The end sections placed on either side of the centre portion, are each 1.9 cm. long with 2,500 turns wound in opposite

directions to produce zero net magnetic moment for the primary when viewed from a distance. In actual operation the primary will have to be kept immersed in liquid helium (it will have then a resistance of 10 ohms and inductance 3.6 henry). One gets an idea about the coil from the data that the primary has a field configuration, at 100 mA, of a maximum of + 30 Gauss at the centre and - 12 Gauss at a point 4.06 cm. from the centre.

Using these data the sensitivity of this coil system about the null point is reported to be 3 Volts/mm for a 250 Hz, 100 mA primary current. With a good transformer and a phase-sensitive-detector off-null voltages of about  $10^{-10}$  Volts can be detected to result in a sensitivity better than 0.1 Å.

### (c) Mutual-Inductance Bridge

When the secondary coil of the variable-transformer described above is slightly displaced from the null position, the coupling between the primary and secondary changes. To measure these changes in coupling a mutual-inductance bridge is necessary. The one used by Sparks & Swenson was (Fig. 2.12), basically a combination of ratio-transformers (Gertsch Model 1011 R) having an open secondary input impedance of 300 Kohms at 250 Hz, a least count of  $10^{-7}$  and a linearity of  $10^{-6}$ . The ratio-transformers (Fig. 2.12) divide the fixed coupling between the primary and the "pick-up" coil. The "pick-up" coil, having 1000 turns and a resistance of 6.5 ohms at 4°K, is wound directly over the various sections of the primary in the proper directions.

While the primary and the secondary circuits are tuned to annul completely their reactance part of the impedance network, the out-of-phase signals are balanced by means of the resistance network. A highly stable oscillator (stable in frequency and output) is used to work the bridge. Because of its linear response for relatively large ranges of displacement ( $\pm 1$  mm) of the secondary of the variable transformer the ratio-transformer may be calibrated for its settings versus displacement directly. A micrometer slide (reading  $10^{-3}$  mm) is used for this purpose. To enable tuning the bridge below 0.1 Å of the secondary coil displacement, a second ratio-transformer (RT2) is used whose output is reduced by a factor of  $10^{-3}$  using a stepdown transformer. Once a rough balance is achieved by means of RT-1, then for a typical thermal expansion measurement only RT-2 settings are varied.

To avoid unwanted noise reaching the detector system, the pyrex glass Dewars have to be supported by inflated-rubber tubes. The reported precision in the measurement of temperature differences was about  $10^{-3}$ °K.

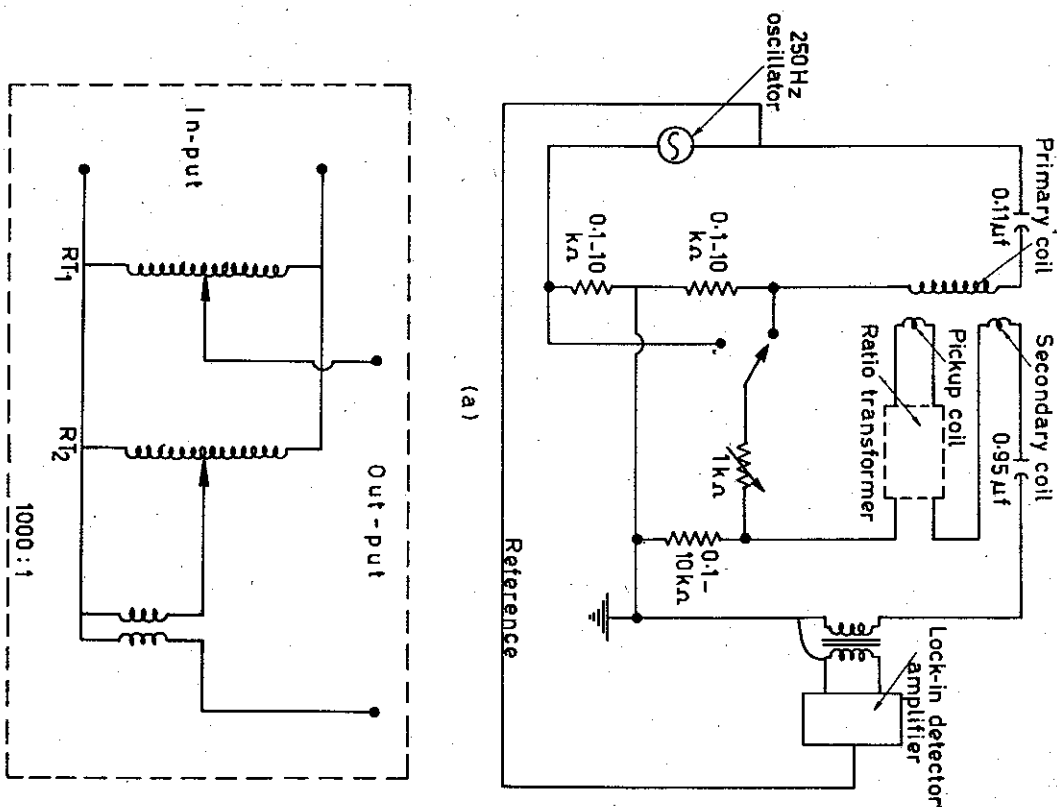


Figure 2.12.

### 2.3.6. Optical Interferometric Techniques

Interferometric methods are most widely used, even today, for the measurement of  $\alpha$  of several materials in various laboratories. This method is based on the principle of converting the variations of the length of the specimen into variations of the optical path difference between the monochromatic interfering light beams, in such a way as to produce a shift in interference fringes with respect to a reference mark in the field of view. There are a few different methods of interferometry that are in vogue in these dilatometers.

#### (a) Fabry-Perot Interferometric Dilatometer

In this method the interference occurs between Fabry-Perot plates. One such device has been used by Bottom (123) to detect displacements as small as  $10^{-7}$  cm. or less. The measurements are made directly in terms of wavelength of the light used. Frazer & Hollis Hallett (357) using this interferometry utilized the observed interference pattern to calculate the length of the etalon spacer (i.e., specimen) at fixed temperatures by the classical method of fitting the integral order numbers. Meincke & Graham (718, 719) used a dynamical method by continuously monitoring the intensity of the central interference fringe by a photo-multiplier. Another version of interferometer which can be incorporated in a dilatometer has been described recently by Kinzly (547). Absolute determinations of  $\alpha$  have been reported using a laser beam of good stability (1426, 1427).

#### (b) Polarized Beam Interferometer

Lebesque et al. (629) employ two quarter-wave plates in the two etalons. Roberts (1650) has described a polarization interferometer for absolute measurements, having a sensitivity of  $10^{-8}/^\circ\text{K}$  at high temperatures.

#### (c) Fringe Width Dilatometer

The principle (Priest, 864) is that the expansion of the solid causes a change in the angle of the wedge formed by the interferometer plates and hence the width of the fringes will be altered. A count of the number of fringes within two fixed marks on one of the plates yields the expansion of the specimen. A single spacer was used in this interferometer. This method has found little application so far.

A version of this technique was developed by Ballard and coworkers (55, 56, 143) to measure thermal expansions of many optical materials.

The disadvantage with this technique is that measurements could not be taken at a stretch for wide temperature ranges because at a higher temperature one fringe will completely occupy the field of view. Therefore the range of study will be restricted to around  $100^\circ\text{C}$  in the case of materials whose  $\alpha \approx 20 \times 10^{-6}/^\circ\text{K}$ .

#### (d) Dilatometer Working on the Interferometric Fringes of the Haidinger Type

In this method the "fringes of equal inclination", produced by a point source of monochromatic light located at infinity, is achieved among the rays reflected between two optical surfaces. Here the specimen is used to support a fused quartz plate (called lower plate) and the upper quartz plate is maintained in a fixed position. The two optical surfaces can be placed at a short distance (as small as 1/10 mm) maintaining a high contrast of the fringes. The upper plate can be aligned, by means of a screw system, so that its lower surface is parallel to the upper surface of the lower plate. Thus a circular fringe pattern will be obtained in the field of view. The specimens can be as long as a few centimetres enabling high accuracy.

Variations of the length of the specimen produce variations of the order of interference in the plane of localization of the fringes. If  $L$  is the length of the specimen, and  $N$  is the order of the interference, we have

$$2\mu L = N\lambda$$

$$\therefore \Delta L = \frac{\lambda}{2} \Delta N \quad (2.3.6)$$

where  $\mu = 1$  for free space.

This relation connects the variations in  $L$  and  $N$ .  $N$  is evaluated by counting the fringes that pass across the centre of the Haidinger fringe system when the temperature of the interferometric assembly is varied. The accuracy of this method depends primarily on the length of the specimen as well as the limit of detection of a fraction of the fringe shift. By using a laser source and by coating the reflecting surfaces by suitable materials, the accuracy can be enhanced.

This method has been used in several laboratories. Of these, Rubin et al. (920) used the interferometer in which the specimen was directly supporting the lower plate unlike those of Barson et al. (73) and Meyerhoff & Smith (728). Fig. 2.13 illustrates schematically the system similar to the one used by Barson et al. (73). The dilatation is obtained with an accuracy of 1% (Barson et al., 73). The peculiarity of these latter versions (Barson et al., 73; Meyerhoff & Smith, 728) is that the interferometric

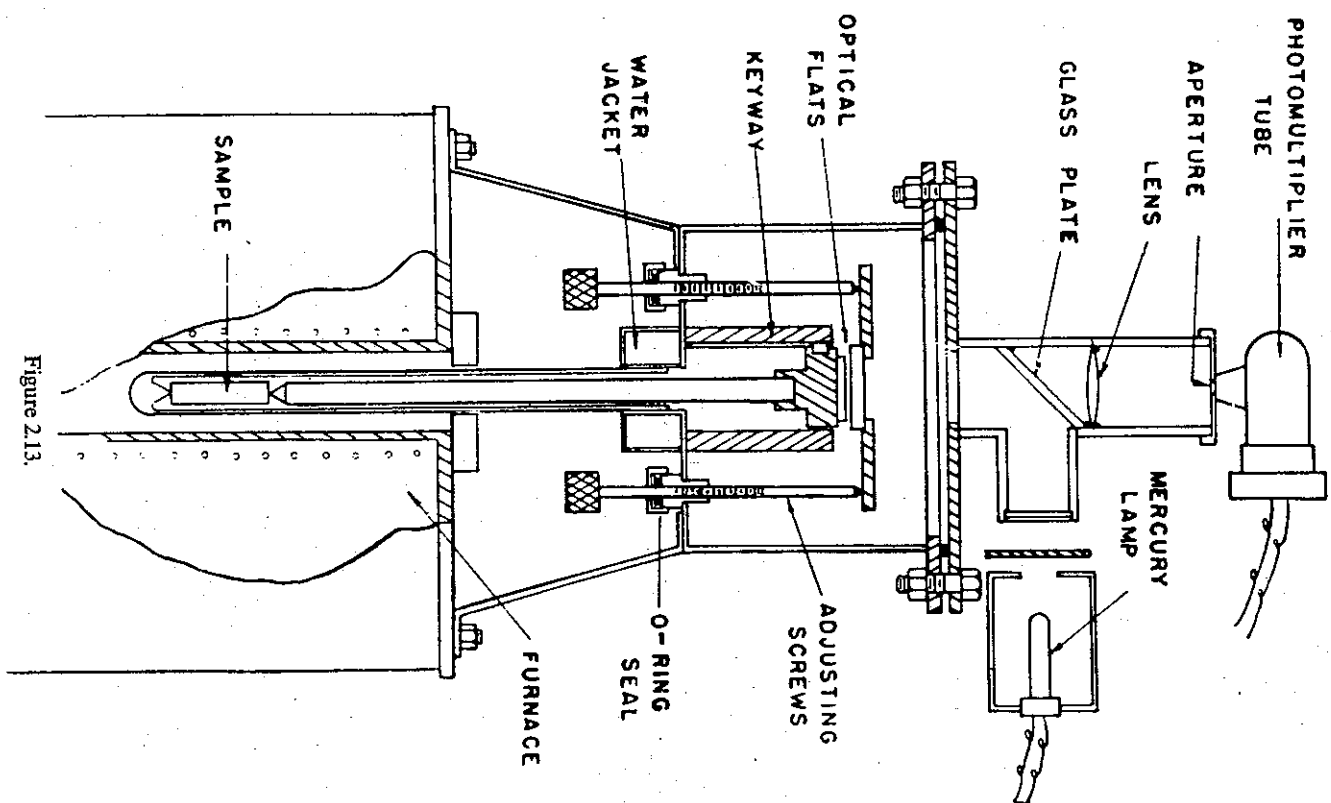


Figure 2.13.

chamber is maintained at constant room temperature, unlike that in Rubin et al. (920). Therefore depending upon the design of the dilatometer, one gets relative or absolute values of  $\alpha$ . (A dynamic measurement of  $\alpha$  is possible in all these methods). Therefore dilatations can be obtained when the specimen is taken to very high temperatures ( $\sim 1000^\circ\text{C}$ ) as well as low temperatures with two different arrangements to heat the specimen.

#### (e) Fizeau's Interferometric Technique

One of the precise optical methods available at present to measure thermal expansion of solids both at low and high temperatures is the interferometric method devised by Fizeau (328, 329). With the ever increasing demand for more accurate knowledge of the properties of matter, at higher temperatures particularly, the original apparatus (i.e., the fundamental method) has passed through a number of modifications in its adaptation to various uses as in the following references: The method of Abbe (1) and Pulfrich (870, 871, 872, 873) was employed by many investigators including Valentiner & Walbot (1104) and Adenstedt (4). Ayres (47) modified the apparatus by using a ring specimen with three conical projections at the top and bottom to measure absolute values of  $\alpha$ , as also by Enck & Dommel (295). A further modification was made by Peters (836).

This interferometric method makes use of the fringes of Fizeau, otherwise known as "fringes of equal thickness or spacing", produced by an extended source of monochromatic light placed at a finite distance, in particular, on a plane. Here the interference between the rays reflected by two optically plane surfaces separated by the specimen are straight fringes.

Several types of spacers are described by Saunders (943). The "three-pin" method which is a further modification by Peters (836) was used extensively by Merritt (725), Saunders (943), Uffelmann (1101), Austin (42), Nix & MacNair (777), Work (1163), Ruffino (923), Press (860), Sreedhar (1026), etc.

Three separate pins are ground in the form of rectangular pyramids (cones, tetrahedra) with pointed tips and a few square mm. in basal area and a few mm. in height (2 to 10 mm), but equal in thickness to within a few wavelengths of the light used ( $< 20 \lambda$ ). These pieces are placed between two fused quartz plates of optical quality, so as to be at the corners of an equilateral triangle. Interference fringes will be obtained when a parallel beam of monochromatic light falls on it. When this interferometer assembly is heated, the elongation  $\Delta L$  in the length





without much delay. Therefore dynamic measurements can be made without much error.

(3) The specimens can be irregular in shape, a feature of great value in dealing with very hard materials.

(4) The apparatus having no moving mechanical parts possesses an unusual simplicity in constructions.

(5) A large number of observations can be made during any single run. Expansion data covering the temperature range based on as many points as the operator desires are easily obtained from a single experiment. The ability to follow the expansion more or less continuously is of particular value when the substance undergoes a phase transition.

(6) Anisotropic materials can be studied fully.

(7) Absolute measurements of high precision are obtained.

#### (g) Disadvantages

(1) The method requires the special and continuous attention of the observer throughout the experiment, which may last 4 to 8 hours and is tedious.

(2) With small metallic specimens, oxidation often occurs at high temperatures. This requires evacuation of the interferometer chamber.

(3) There is the necessity of making a correction for the variation with pressure and temperature of the refractive index of air. (A vacuum of  $100 \mu$  will be sufficient to eliminate corrections for index changes.)

### 2.3.7. Dilatometer With Grids

In this method the working principle of the apparatus is the transformation of changes of length into changes of light intensity. The light is passed through two closely spaced grids, one of which is held fixed, and the other is attached to the free end of the specimen (in the form of a small bar) whose expansion is to be determined. One grid is regular and the other has an irregularity in the middle as shown in Fig. 2.15. Such a grid system has been described earlier by Jones (512).

Thus the changes in output of two differentially connected photocells placed behind the two halves of the grids will give a linear function of the grid displacement. If the relative position of grids is varied due to the dilatation of the specimen then a neat trace will be obtained in a recorder. The accuracy of measurement is claimed to be of the order of  $10^{-8}$  cm. (Andres, 14). This method is not a popular one as it stands today. The only laboratory which makes use of this technique for thermal expansion is that of Andres who developed this technique. A few metals have been

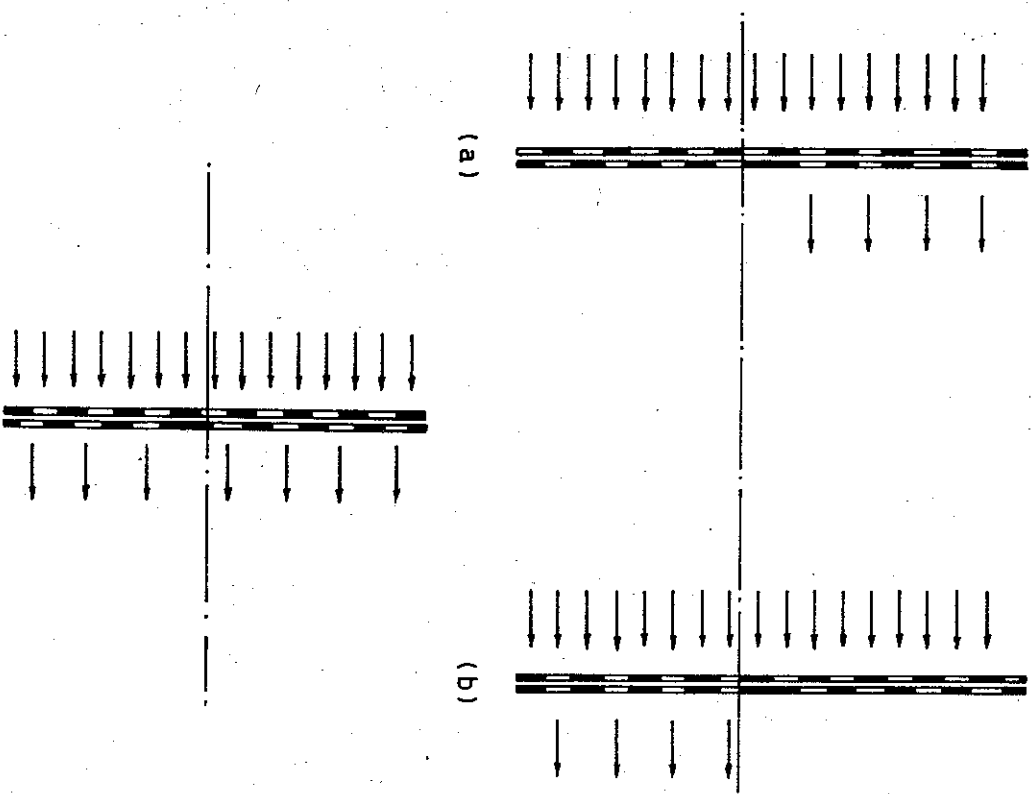


Figure 2.15.

(working principle of grids).

(a) no light can pass through the lower half of the grids.

(b) the second grid is displaced by one line width with respect to the first and the situation of (a) is reversed.

(c) when the grids are in any other position than (a) or (b) both the halves of the grids are equally transparent.

studied by this method by Andres (15, 16, 17, 18, 20) and Andres & Rohrer (21).

The method described above can be used for moderately long samples (a few cms.). But it yields only relative values of  $\alpha$  because the measurements are with respect to the material supporting the specimen.

### 2.3.8. Other Methods

There are a few other methods for the determination of thermal dilatation, and these cannot be classified in any of the groups described earlier.

(a) Thermal expansion can be estimated for solids by determining the stress coefficients of electrical resistance of the material. This is an entirely different method (1701), and is based on the simultaneous measurement of the resistances of two identical wires (of the material) of which one is stretched relative to the other by longitudinal stresses. Though as a method this is all right for an evaluation of  $\alpha$  the precise knowledge of other physical quantities like the Poisson's ratio, Young's modulus, density, specific heat of the material is indispensable for calculations using the adiabatic and isothermal stress coefficients of resistance measured. This indirect method has not therefore attracted many investigators.

(b) Mäntysalo (671, 672) has made use of an "ultrasonic microwave" apparatus for the measurement of thermal expansion of lithium crystal. It consists essentially of an ultra-high-frequency (UHF) acoustic transmission probe and an UHF spectrometer. An amplitude modulated UHF oscillator and a signal amplifier constitute an ultrasonic continuous wave spectrometer. The amplitude modulated UHF energy is fed into the transmission line. When this energy is transferred into the resonance probe a transducer converts it into ultrasonic energy. These longitudinal ultrasonic waves are propagated through the specimen, of a single crystal, and cause a flow of heat accompanied by a dissipation of ultrasonic energy. In other words, attenuation of the amplitude of ultrasonic waves takes place in the crystal. A second transducer converts the attenuated signal back into UHF signal. This forms the input for a narrow band amplifier and a phase sensitive detector system. The d.c. output is then traced in a recorder to get a curve which is the result of the amplitude variation of the UHF signal. Fig 2.16 shows the block diagram of the ultrasonic dilatometer apparatus.

Due to thermal expansion the crystal expands and under appropriate conditions resonance occurs and standing waves are set up. The result

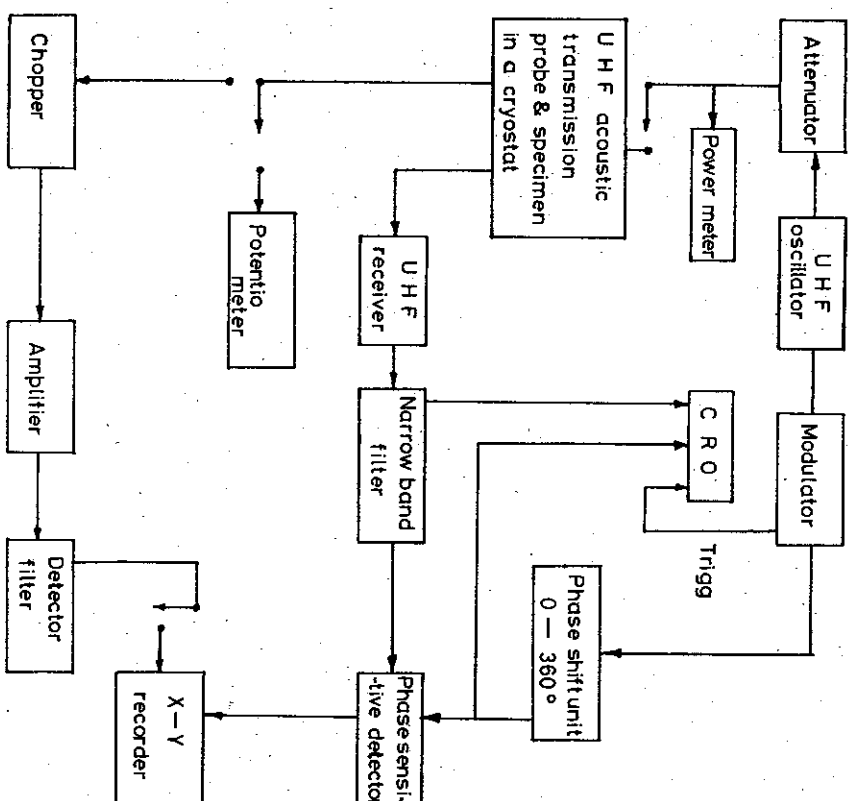


Figure 2.16.

will be an oscillating curve of the ultrasonic attenuation as a function of temperature. The period of oscillation of this curve is given by

$$\Delta T = \frac{\lambda}{2l_T \alpha} \quad (2.3.11)$$

or,

$$\alpha = \frac{v_T}{2l_0 \Delta T} \quad (2.3.12)$$

where  $\lambda$  is the wavelength of the UHF wave,  $l_r$  is the length of the specimen at temperature  $T^\circ\text{K}$ ,  $\nu$  is the UHF frequency,  $v$  is the velocity of the UHF wave. The accuracy of  $\alpha$  obtained by this *Ultrasonic Microwave* method is greatly limited by the errors in the determination of  $\nu$  and  $T$ . Mäntysalo (671, 672) reported the value of  $\alpha$  for lithium within an error of  $\pm 0.5 \times 10^{-6}/^\circ\text{K}$ . If the temperature is measured very precisely, the author is hopeful of an accuracy of  $10^{-8}/^\circ\text{K}$  with this method.

(c) For the sake of completeness it is necessary to mention the other dilatometers that have been found in the literature. They are: silicon carbide dilatometer (Mark & Emmanuelson, 683), a precision direct reading dilatometer (Verhaeghe et al. 1116), a vacuum contact dilatometer (Gumenyuk, 421), quartz dilatometer (Henning, 441), Totskii (1087), dilatometer using a coaxial resonator with capacity loading for 9.5 GHz as the sensor (Pudalov & Khaikin, 868), a differential photorecording Chevenard dilatometer (Chevenard, 177, Arbutov & Zelenkov, 25, 26, and Mironov et al., 735), quartz dilatometer of Strelkov type used by many Russian investigators (Strelkov et al., 1059), (Kobyakov & Smolenko, 563), (Kovalevskaya & Strelkov, 572, and Amatuni & Shevchenko, 22, Manzheli & Tolkachev, 675), and Gaertner dilatation interferometer model I-1118t used by Cook (201, 203).

### 2.3.9. Automatic Registration of Dilatation by Different Techniques

In order to avoid the strain to the observer in making dilatometric measurements, many investigators resorted to automatic recording of thermal expansion data. As it is found unnecessary to describe them, only the different references with a brief mention of the techniques will be given. A differential dilatometer with *mechanical registration* was reported by Chevenard (176, 177). Interferometric dilatometer employing *automatic photography* by Sinden (996) and dilatometers based on the work on the photography of moving interference fringes by Troubridge (1090), Arnulf (34), Couët et al. (208) and Nix & McNair (776) were used in the earlier stage of development of automatization. *Automatic recording of the movement of fringes* in an interferometric dilatometer was first introduced by Vernon & Weintraub (1118) with a photomultiplier, and this principle was subsequently used in many laboratories by Work (1163), Green et al. (408), Meyerhoff & Smith (728), Enck & Dommel (295), Channing & Weintraub (170, 171), Devanarayan (257), etc. Ruffino (923, 924) used an interferometric dilatometer with *electronic fringe counter* based on the displacement of a fringe which modulates the luminous flux incident on a photomultiplier, whose output has an a.c. component that activates a Smith's circuit. A high temperature recording

dilatometer using a different principle employing two photovoltaic cells has been reported by Liberman & Gandall (641). A linear *variable displacement transducer* and a silica push-rod system have been incorporated in an automatic dilatometer by Abell et al. (1187, 1188). Other references on automatic dilatometers are also available, for e.g., Bowles & Sugarman (126), McDonald & Pinkney (705). Variations in the values of interplanar spacing and the expansion coefficient with temperature in an X-ray diffractometer were automatically recorded in the method used by Shimura (987, 988).

### 2.4. RECENT EFFORTS TO STANDARDIZE THERMAL EXPANSION MEASUREMENTS:

In the last decade, it was accepted by most of the laboratories to refer to Magnesium Oxide (MgO) as a standard material for thermal expansion. Accordingly, thermal expansion measurements on MgO were carried out by different methods and also by the same technique by various laboratories. Later the following eight materials have been adopted by the National Bureau of Standards as standard reference materials (SRM) for thermal expansion. They are: Copper, Tungsten, Stainless Steel, an Aluminum Alloy, Graphite, Vitreous Silica, Borosilicate Glass and Sapphire Single Crystal. SRM-736 is copper, and this is available by placing an order with the Office of Standard Reference Materials, NBS, Washington, D.C. 20234. SRM-736 is available in the form of a rod  $1/4''$  diameter and in 2-, 4-, and 6" lengths.

Thermal expansion data of copper (SRM-736) have been measured by means of Fizeau's interferometric method between 20 to 800°K, recently by Hahn (1388). Other members of the series of materials certified as thermal expansion standards by the NBS are fused silica (SRM-739) and platinum, and the expansion data of these materials have been reported (1389, 1390). The structure and materials panel of AGARD (Advisory Group of Aerospace Research and Development) has started a co-operative measurement programme in 1967 (1345) concerning thermophysical properties of solids at high temperatures. This programme aims at estimating absolute accuracy of thermophysical property data and to indicate the best way of obtaining accurate results. Many laboratories have contributed results up to 1000°C for materials like pure gold and platinum (1346, 1347, 1348), McLean et al. (1529) studied copper, silver and gold below 30°K in the same year when White & Collins (1801) reported their values. Measurements on tungsten SRM 737 (density  $19.2 \text{ Mg m}^{-3}$ ) have been made by Kirby & Hahn (quoted by Roberts, 1650).

### 2.5.1. Reduction of the Observations on Thermal Expansion of Anisotropic Crystals in Terms of the Principal Axes of the Expansion Ellipsoid

As was pointed out in Chapter 1, crystals in general exhibit thermal anisotropy; that is, the expansion coefficient is different in different crystallographic directions. A perusal of Table 1.1. will show that it becomes necessary to measure in the case of crystals all the independent coefficients of the general second-rank tensor,  $\alpha_{ik}$ . The thermal expansion tensor, when referred to in terms of its *principal axes*, takes the form,

$$[\alpha_{ik}] = \begin{bmatrix} \alpha_1 & 0 & 0 \\ 0 & \alpha_2 & 0 \\ 0 & 0 & \alpha_3 \end{bmatrix} \quad (2.5.1.)$$

Here  $\alpha_1$ ,  $\alpha_2$  &  $\alpha_3$  are known as principal expansion coefficients which are in general different from  $\alpha_{11}$ ,  $\alpha_{22}$  and  $\alpha_{33}$ , respectively. The volume coefficient of thermal expansion  $\beta$  is given by

$$\beta = \alpha_1 + \alpha_2 + \alpha_3 \quad (2.5.2.)$$

In order to fix the orientation of the thermal expansion ellipsoid with respect to the crystallographic axes, the first step should be to find out the thermal expansion tensor. Secondly, it is necessary to determine the principal coefficients of expansion so as to enable it to be expressed in the standard tensor form. In the case of crystals belonging to the tetragonal, hexagonal and orthorhombic systems, the directions of the principal values of  $\alpha$  coincide with those along the crystallographic axes. Thus, for orthorhombic crystals,  $\alpha_1 = \alpha_a$ ,  $\alpha_2 = \alpha_b$ ,  $\alpha_3 = \alpha_c$ , where subscripts  $a$ ,  $b$  &  $c$  denote the directions along the crystallographic axes. On the other hand, crystals belonging to the tetragonal and hexagonal systems,  $\alpha_1 = \alpha_2 = \alpha_a$  and  $\alpha_3 = \alpha_c$ , where  $c$  is the unique axis of the crystal. In the case of triclinic and monoclinic crystals the situation is different and therefore they will be dealt with separately in the following section.

### 2.5.2. To Find out $\alpha_{11}$ , $\alpha_{22}$ , $\alpha_{33}$ and $\alpha_{31}$ by a Least Squares Procedure in the Case of Monoclinic Crystals

Nye (1957) has given a least squares procedure due to W.L. Bond. This has been illustrated clearly in the case of monoclinic sodium selenite  $[\text{NaH}_3(\text{SeO}_3)_2]$ , by Devanarayana (257). A monoclinic crystal will have one of its principal axes ( $\alpha_2$ ) of the thermal expansion ellipsoid coinciding with the crystallographic  $b$ -axis, and the other two principal axes are not fixed by symmetry considerations. The orientation of these

two principal axes in the (010) plane is governed by the actual structure of the crystal and can be determined experimentally by measurements along three arbitrary directions in the (010) plane. Thus measurements along 4 different directions including the unique axis direction are necessary to describe the ellipsoid. Let  $x$ ,  $y$ , and  $z$  be the three directions in the (010) plane such that the angles  $\xi_1$ ,  $\xi_2$  &  $\xi_3$ , respectively, defining these directions with respect to, say, the crystallographic  $c$ -axis, are known. One can then form the operator  $\xi$ , designated in matrix notation as

$$[\xi] = \begin{bmatrix} \sin^2 \xi_1 & \sin 2\xi_1 & \cos^2 \xi_1 \\ \sin^2 \xi_2 & \sin 2\xi_2 & \cos^2 \xi_2 \\ \sin^2 \xi_3 & \sin 2\xi_3 & \cos^2 \xi_3 \end{bmatrix} \quad (2.5.3.)$$

If  $[\xi]_t$  is the transpose of  $[\xi]$  one can find out the determinant  $\Delta = |[\xi]_t[\xi]|$  and the inverse  $([\xi]_t[\xi])^{-1}$  so as to find out the transformation matrix,  $[T]$ .

$$[T] = ([\xi]_t[\xi])^{-1}[\xi]_t \quad (2.5.4.)$$

Then it will be possible to find out the expansion coefficients by means of the equation

$$\begin{bmatrix} \alpha_{11} \\ \alpha_{31} \\ \alpha_{33} \end{bmatrix} = [T] \begin{bmatrix} \text{Value of } \alpha \text{ along } x = \alpha_x \\ \text{Value of } \alpha \text{ along } y = \alpha_y \\ \text{Value of } \alpha \text{ along } z = \alpha_z \end{bmatrix} \quad (2.5.5.)$$

The right hand side of equation (2.5.5.) will yield the values  $\alpha_{11}$ ,  $\alpha_{31}$  and  $\alpha_{33}$ .

After finding out the values of the tensor components of the expansion ellipsoid, given by

$$\begin{bmatrix} \alpha_{11} & 0 & \alpha_{31} \\ 0 & \alpha_{22} & 0 \\ \alpha_{31} & 0 & \alpha_{33} \end{bmatrix}$$

It is necessary to fix the orientation of this ellipsoid with respect to the crystallographic axes. For this the magnitude of the principal expansion coefficients  $\alpha_1$  and  $\alpha_3$ , and the angle  $\varphi$  have to be determined. The parameter  $\varphi$  relates one of these principal coefficients with a crystallographic axis in the (010) plane.  $\varphi$  can be determined by using the Mohr circle construction as follows:

Letting the  $\alpha_3$  axis inclined at an angle  $\varphi$  measured counter-clockwise to the  $c$ -axis, then

$$\tan 2\phi = \frac{2|\alpha_{31}|}{\alpha_{33} - \alpha_{11}} \quad (2.5.6)$$

If  $r_M$  is the radius of the Mohr circle,

$$r_M^2 = \frac{1}{4}(\alpha_{33} - \alpha_{11})^2 + \alpha_{31}^2 \quad (2.5.7)$$

This yields

$$\alpha_1 = \frac{1}{2}(\alpha_{11} + \alpha_{33}) - r_M \quad (2.5.8a)$$

$$\alpha_3 = \frac{1}{2}(\alpha_{11} + \alpha_{33}) + r_M \quad (2.5.8b)$$

Thus the four parameters, viz.,  $\alpha_1$ ,  $\alpha_3$ ,  $\phi$  [from equations (2.5.7) and (2.5.8)] and  $\alpha_2$  can be computed. It is but proper to mention here that the literature indicates that thermal expansions of only a few monoclinic crystals have been thoroughly investigated so far.

### 2.5.3. To Find out the Orientation of the Expansion Ellipsoid for Triclinic Crystals

A perusal of the literature indicates that there is striking lack of information about crystals belonging to the triclinic system. Only three crystals of this system are known to have been studied for thermal expansion in detail (Boric acid, 653; Furoic acid, 708; and Copper sulphate, 1027).

The number of independent experimental measurements necessary for a triclinic crystal is six (Table, 1.1). It is, therefore, necessary to perform expansion measurements along six general directions fixed with respect to the crystal axes so as to define completely the expansion ellipsoid. The magnitude of the principal coefficients of expansion and the orientation with respect to the crystal axes can be obtained by using the method given by Sreedhar (1027) or by the generalized matrix method treated by Nye (1575). Unlike in the case of a monoclinic crystal, both the operators  $[\xi]$  and  $[T]$  will be more complicated for a triclinic crystal.  $\alpha_{ik}$  is given by

$$\begin{bmatrix} \alpha_{11} \\ \alpha_{22} \\ \alpha_{33} \\ \alpha_{32} \\ \alpha_{31} \\ \alpha_{21} \end{bmatrix} = [T] \begin{bmatrix} \text{Value of } \alpha \text{ along direction } l \\ \text{Value of } \alpha \text{ along direction } m \\ \text{Value of } \alpha \text{ along direction } n \\ \text{Value of } \alpha \text{ along direction } p \\ \text{Value of } \alpha \text{ along direction } q \\ \text{Value of } \alpha \text{ along direction } r \end{bmatrix} \quad (2.5.9)$$

where  $l, m, n, p, q$  &  $r$  define the six directions along which the values of

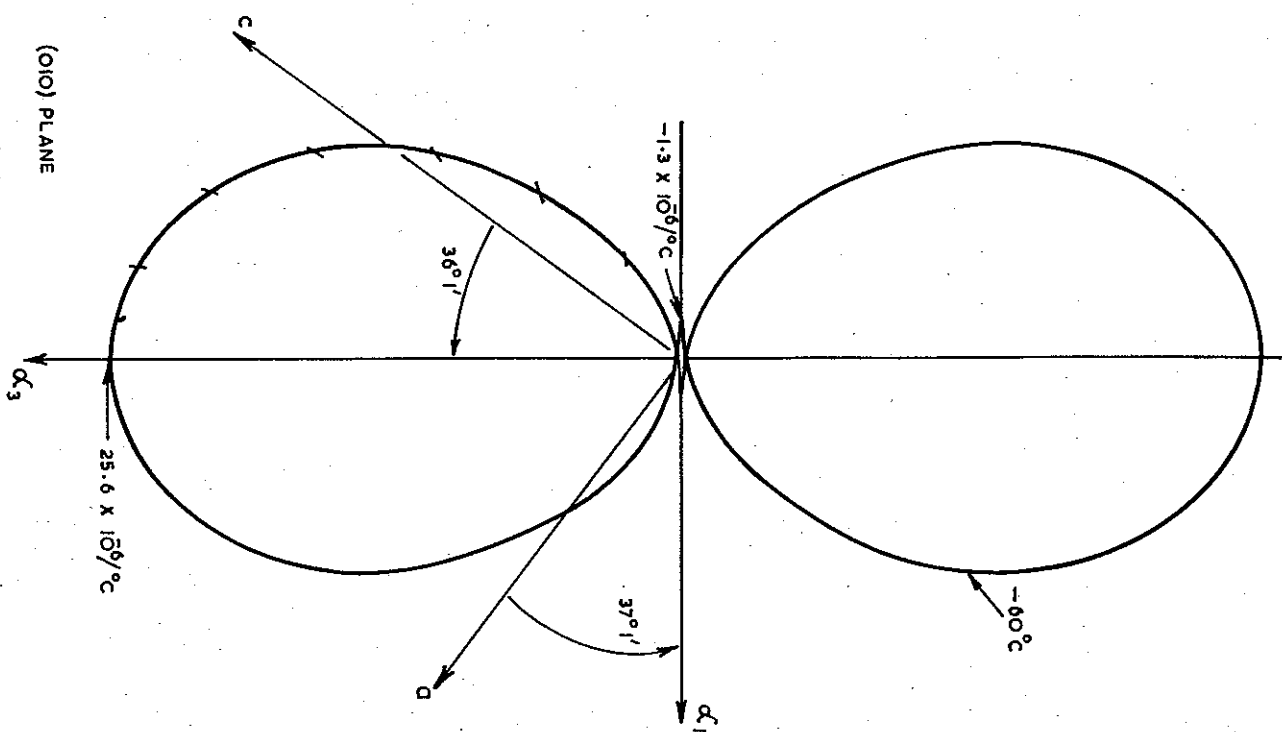


Figure 2.17. Polar Diagram of  $\alpha$  of  $\text{NaH}_2(\text{SeO}_3)_2$ .

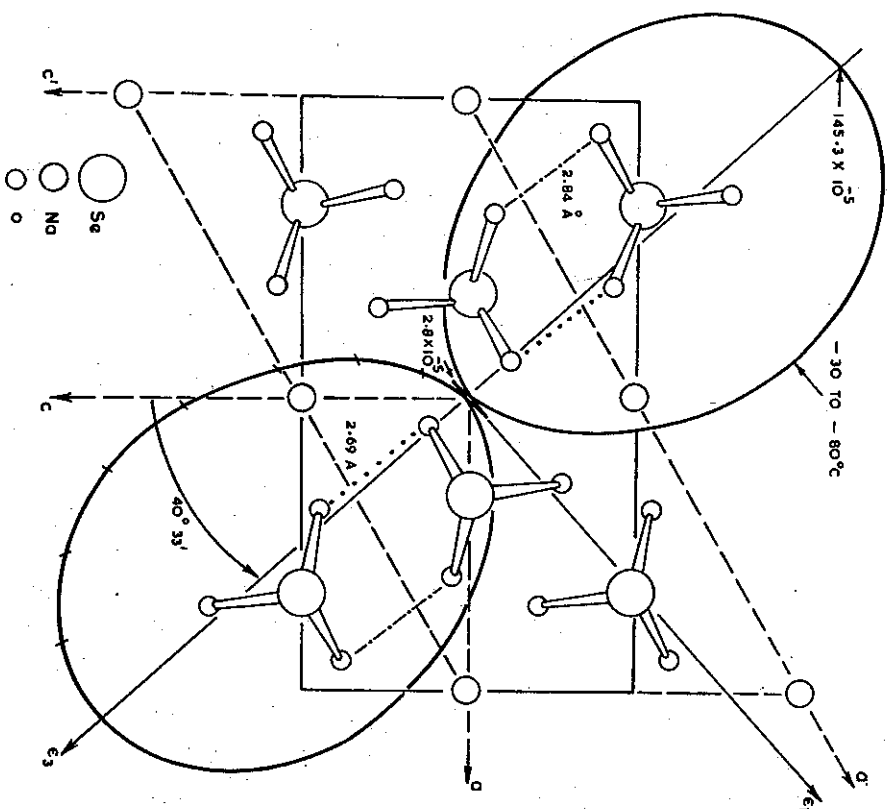


Figure 2.18. Variation of Thermal Dilatation  $\epsilon$  with Orientation Superposed on the Crystal Structure of  $\text{NaH}_3(\text{SeO}_3)_2$ .

$\alpha$  have been determined, and whose orientations are described by [5]. The principal coefficients and the other three parameters can be evaluated from the  $\alpha_{ik}$  values using a method of successive approximation (Nye, *loc. cit.*).

## 2.5.4. The Voigt Relation

Once the values of  $\alpha_1$ ,  $\alpha_2$  and  $\alpha_3$  for a crystal belonging to an anisotropic system are known then one can find out the value of  $\alpha$  for any desired

direction in the crystal by making use of a relation, commonly known as the *Voigt relation*,

$$\alpha_\psi = \alpha_{11} \cos^2 \psi + \alpha_{\perp} \sin^2 \psi = \alpha_{\perp} + (\alpha_{11} - \alpha_{\perp}) \cos^2 \psi \quad (2.5.10)$$

where

$$\alpha_{11} = \alpha_3 \text{ for } \psi = 0^\circ,$$

and

$$\alpha_{\perp} = \alpha_1 \text{ for } \psi = 90^\circ.$$

$\alpha_\psi$  is the value along the direction which makes an inclination  $\psi$  to the axis corresponding to  $\alpha_3$ , and lying in the plane containing  $\alpha_1$  and  $\alpha_3$ .

In order to find out the correlation, if any, that may exist between the thermal expansion and the crystal structure, it becomes necessary to represent the thermal expansion by means of a 'polar diagram'. Polar diagrams are generally drawn for a particular temperature in a particular plane. Fig. 2.17, (260, 588) is illustrative of this. But polar diagrams of thermal expansion coefficient in a plane may not be sufficient. To give a better picture and correlation between the structure of the crystal and its thermal expansion, few authors resort to polar diagrams of 'thermal strain' rather than thermal expansion coefficient, in such a way that they are superposed on the projections of the crystal structure in the corresponding planes. Fig. 2.18, illustrates the variation of the thermal dilatation with orientation superposed on the structure of monoclinic  $\text{NaH}_3(\text{SeO}_3)_2$  in the (010) plane, as given by Devanarayanan (257), and referred to in the literature (260, 588). Similar attempts have been made in the case of few other crystals also (8, 258, 368, 707, 1097, 1098, 1099, 1652, etc.). Anisotropy of thermal expansion is a result of the anisotropy of the intermolecular forces, and has its origin in the distribution of the particular type/types of bonds within the given crystal.

## CHAPTER 3

## Theory of Thermal Expansion of Crystals

## 3.1. LATTICE CONTRIBUTION TO THERMAL EXPANSION

The normal modes of vibration of a crystal lattice are plane waves in the *harmonic approximation*. Each wave is characterised by a wave vector  $\vec{q}$  and a frequency  $\omega_j(\vec{q})$ . If there are  $p$  atoms in the unit cell of the crystal, there are  $3p$  different normal modes denoted by the index  $j$  running from 1 to  $3p$ . Of the  $3p$  branches  $\omega_j(\vec{q})$ , there are 3 branches,  $j = 1, 2, 3$ , which correspond to the elastic waves propagated in the lattice in the limit of long wavelengths ( $\vec{q} \rightarrow 0$ ). In this limit of long waves, the different atoms in the unit cell move in unison in these modes. The remaining  $3p - 3$  branches are called optical branches. In the long wave limit, these modes of vibration correspond to the motion of the  $p$  sublattices one against the other. These are the frequencies which appear in the Raman and Infrared absorption spectra of the crystal. When we deal with a finite crystal having  $N$  unit cells the boundary conditions allow only  $N$  values of the wave vector  $\vec{q}$  in the Brillouin zone. These allowed wave vectors are denoted by a subscript  $i$  to  $q$ . There are, therefore,  $3pN$  normal modes of oscillation of the crystal lattice with frequencies  $\omega_j(\vec{q}_i)$  ( $j = 1, \dots, 3p; i = 1, \dots, N$ ).

In the *harmonic approximation* there can be no thermal expansion. The atoms vibrate about their equilibrium positions symmetrically whatever be the amplitude. To account for the thermal expansion one has to take into account the *anharmonicity* of the lattice vibrations. The simplest and most convenient way to do this is to assume that the harmonic approximation is valid for every volume of the crystal, but the frequencies of vibration are dependent on the volume. This approximation is called the *quasi-harmonic approximation* and can be used as long as the temperature  $T \ll \Theta$ , where  $\Theta$  is the equivalent Debye temperature of the crystal. The quasi-harmonic approximation provides the most convenient method for discussing the thermal expansion of a crystal at moderate temperatures. The reason for the success of the quasi-harmonic approximation will be discussed in a later section. The first detailed theoretical

discussion of thermal expansion on this basis was given by Barron (64). Barron's work stimulated considerable experimental and theoretical research in the last decade on the thermal expansion of crystals.

In the quasi-harmonic approximation a normal mode of frequency  $\omega_j(\vec{q}_i)$  has a free energy associated with it. This free energy  $f_{j,i}$  is given by

$$f_{j,i} = kT \left\{ \frac{1}{2} x_{j,i} + \ln [1 - \exp(-x_{j,i})] \right\} \quad (3.1.1)$$

where  $k$  is the Boltzmann's constant,  $T$  is the temperature in degrees Kelvin and

$$x_{j,i} = \hbar \omega_j(\vec{q}_i) / kT \quad (3.1.2)$$

where  $\hbar$  is the Planck's constant.

The total free energy  $\mathcal{F}(T, V)$  due to all the normal modes of vibration is given by

$$\begin{aligned} \mathcal{F}(T, V) &= \sum_{j=1}^{3p} \sum_{i=1}^N f_{j,i} \\ &= kT \sum_{j=1}^{3p} \sum_{i=1}^N \left\{ \frac{1}{2} x_{j,i} + \ln [1 - \exp(-x_{j,i})] \right\} \end{aligned} \quad (3.1.3)$$

This is a function of temperature and volume. Using the thermodynamic relation

$$S = - \left( \frac{\partial \mathcal{F}}{\partial T} \right)_V \quad (3.1.4)$$

for the entropy, we get

$$S = k \sum_{j=1}^{3p} \sum_{i=1}^N \left\{ \frac{x_{j,i} \exp(-x_{j,i})}{[1 - \exp(-x_{j,i})]} - \ln [1 - \exp(-x_{j,i})] \right\} \quad (3.1.5)$$

The specific heat at constant volume  $C_{\text{vib}}$  in the *harmonic approximation* is

$$C_{\text{vib}} = T \left( \frac{\partial S}{\partial T} \right)_V = k \sum_{j=1}^{3p} \sum_{i=1}^N \sigma_{j,i} \quad (3.1.6)$$

where

$$\sigma_{j,i} = x_{j,i}^2 \exp(x_{j,i}) / [1 - \exp(x_{j,i})]^2 \quad (3.1.7)$$

is the Einstein specific heat function.

From the thermodynamic relation

$$\left( \frac{\partial S}{\partial V} \right)_T = \left( \frac{\partial P}{\partial T} \right)_V = \frac{\beta}{\chi_T} \quad (3.1.8)$$



where  $P$  is the pressure,  $\beta$  is the volume expansion coefficient and  $\chi_T$  is the isothermal compressibility we obtain,

$$\frac{\beta V}{\chi_T} = k \sum_{j=1}^{3p} \sum_{i=1}^N \gamma_{ji} \cdot \sigma_{ji} \quad (3.1.9)$$

where

$$\gamma_{ji} = - \frac{\partial \ln \chi_{ji}}{\partial \ln V} = - \frac{\partial \ln \omega_j(\vec{q}_i)}{\partial \ln V}$$

$\gamma_{ji}$  is called the *Grüneisen parameter for the normal mode* frequency  $\omega_j(\vec{q}_i)$ . This represents the fractional change in the frequency with the fractional change in volume. In the quasi-harmonic approximation the  $\gamma_{ji}$  are non-zero in general and are assumed to be independent of volume and temperature. This latter assumption is not quite justified.

The temperature dependence of the volume expansion coefficient can be expressed most conveniently in terms of the temperature dependence of an *equivalent Grüneisen parameter*  $\gamma_T$  defined by the relation

$$\gamma_T = \frac{\beta V}{\chi_T C_{vhar}} \quad (3.1.11)$$

Substituting for  $\beta V/\chi_T$  and  $C_{vhar}$  we get

$$\gamma_T = \frac{\sum_{j=1}^{3p} \sum_{i=1}^N \gamma_{ji} \cdot \sigma_{ji}}{\sum_{j=1}^{3p} \sum_{i=1}^N \sigma_{ji}} \quad (3.1.12)$$

$\gamma_T$  is, therefore, the *weighted average* over the Grüneisen parameters for the individual normal modes. The weightage factors are the Einstein specific heat functions. Though the  $\gamma_{ji}$  are constants, the Einstein functions are temperature dependent, and this results in a temperature variation of  $\gamma_T$ . Using  $\gamma_T$  to discuss the thermal expansion coefficient  $\beta$  is analogous to the use of a temperature dependent equivalent Debye temperature to discuss the specific heat of a crystal.

From the expression for  $\gamma_T$  we can derive the following conclusions. At very high temperatures (i.e.,  $T \gg \Theta$ ) all the normal modes contribute equally to the specific heat (i.e.,  $\sigma_{ji} = 1$ ). So the equivalent Grüneisen parameter reaches a limiting value,

$$\gamma_\infty = \frac{1}{3pN} \sum_{j=1}^{3p} \sum_{i=1}^N \gamma_{ji} \quad (3.1.13)$$

This limiting value is nothing but the average over the Grüneisen parameters of all the normal modes. As the temperature is reduced the higher frequencies get frozen out. So the Grüneisen parameters for higher frequencies progressively decrease in importance in determining  $\gamma_T$ . When we reach such low temperatures that only the long wavelength elastic waves contribute to the specific heat of the crystal (in this region the molar specific heat  $C_{vhar} = (12/5)\pi^4 k(T/\Theta)^3$ ),  $\gamma_T$  approaches a differing limiting value  $\gamma_0$ .  $\gamma_0$  is given by

$$\gamma_0 = \frac{\sum_{j=1}^3 \sum_{i=1}^N \gamma_{ji} \cdot \sigma_{ji}}{\sum_{j=1}^3 \sum_{i=1}^N \sigma_{ji}} \quad (3.1.14)$$

The optical branches do not contribute to  $\gamma_0$ . In the long wave limit the frequency  $\omega_j(\vec{q}_i)$  of a normal mode belonging to an acoustic branch is given by

$$\omega_j(\vec{q}_i) = s_j(\theta, \varphi) \cdot |\vec{q}_i| \quad (3.1.15)$$

where  $s_j(\theta, \varphi)$  is the velocity of the  $j$ th elastic wave propagating in the direction  $(\theta, \varphi)$  in the crystal.  $s_j(\theta, \varphi)$  can be calculated from the elastic constants of the crystal. The number of normal modes in a solid angle  $d\Omega$  for wave propagation within a frequency range  $\omega$  to  $\omega + d\omega$  in the  $j$ th acoustic branch propagating in the direction  $(\theta, \varphi)$  is proportional to

$$\frac{1}{8\pi^3} \omega^2 d\omega \frac{d\Omega}{s_j^3(\theta, \varphi)} \quad (3.1.16)$$

The summation over  $i$  can be converted into an integration over  $\omega$  and  $\Omega$  and

$$\gamma_0 = \frac{\sum_{j=1}^3 \int \gamma_j(\theta, \varphi) \frac{d\Omega}{s_j^3(\theta, \varphi)}}{\sum_{j=1}^3 \int \frac{d\Omega}{s_j^3(\theta, \varphi)}} \quad (3.1.17)$$

At intermediate temperatures the behaviour of  $\gamma_T$  can be obtained only by numerical computations once the  $\gamma_{ji}$  are known.

Barron (54) showed that the approach of  $\gamma_T$  to the high temperature limit can be conveniently studied in terms of the quantities  $\gamma(n)$  defined as follows.

$$\gamma(n) = - \frac{1}{n} \frac{\partial \ln \mu_n}{\partial \ln V} \quad (3.1.18)$$

where

$$\mu_n = \frac{1}{3Np} \sum_{j=1}^{3p} \sum_{i=1}^N \omega_j^n(q_i) \quad (3.1.19)$$

are the  $n$ th moments of the frequency distribution function for the lattice. Using the definition of  $\mu_n$  we see that

$$\gamma(n) = \frac{\sum_{i=1}^{3p} \sum_{j=1}^N \gamma_{ji} \cdot \omega_j^n(q_i)}{\sum_{j=1}^{3p} \sum_{i=1}^N \omega_j^n(q_i)} \quad (3.1.20)$$

Therefore  $\gamma(n)$  is defined in the range  $-3 < n \leq 0$  and  $n > 0$ . The high temperature limit  $\gamma_\infty$  is given by  $\gamma(0)$  and the low temperature limit  $\gamma_0$  by  $\gamma(-3)$ , where  $\gamma(0)$  and  $\gamma(-3)$  are the limiting values of  $\gamma(n)$  as  $n$  tends to zero and  $-3$ , respectively. Using the Thirring expansion for the Einstein specific heat function  $\gamma_T$  can be expressed in terms of  $\gamma(n)$  and  $\mu_n$ . This expansion is given by equation (3.1.21).

$$\begin{aligned} \gamma_T = \gamma_\infty - T^{-2} & \left\{ \frac{\mu_2^*}{12} [\gamma(2) - \gamma(0)] \right\} \\ & + T^{-4} \left\{ \frac{\mu_4^*}{240} [\gamma(4) - \gamma(0)] - \left( \frac{\mu_2^*}{12} \right)^2 [\gamma(2) - \gamma(0)] \right\} \\ & - T^{-6} \left\{ \frac{\mu_6^*}{6048} [\gamma(6) - \gamma(0)] - \frac{\mu_2^*}{12} \frac{\mu_4^*}{240} [\gamma(4) - \gamma(0)] \right. \\ & \quad \left. + \frac{\mu_2^*}{12} \left[ \left( \frac{\mu_2^*}{12} \right)^2 - \frac{\mu_4^*}{240} \right] [\gamma(2) - \gamma(0)] \right\} \\ & + \dots \end{aligned} \quad (3.1.21)$$

where

$$\mu_n^* = \left( \frac{\hbar}{k} \right)^n \cdot \mu_n$$

This series converges for  $T > 0.2\Theta$ , where  $\Theta$  is the *equivalent Debye temperature* of the crystal. Using the series it should be possible to calculate  $\gamma_T$  down to about  $0.2\Theta$  if the  $\gamma(n)$  and  $\mu_n$  were known. This can be done if one takes a specific model for the forces of interaction between the atoms in the crystal. The advantage of the expansion is that it involves only the even moments of the frequency distribution function which can be obtained by raising the dynamical matrix determining the frequencies to the desired power, taking their trace and then carrying out the averaging

process over the different wave vectors. The convergence of this series can be improved by using an Euler transformation to replace  $T^{-2}$  by

$$t = \left\{ 1 + \left( \frac{T}{T_1} \right)^2 \right\}^{-1} \quad (3.1.22)$$

where  $T_1 \approx 0.2\Theta$  and eliminating  $T$  between the two equations. This transformation was first suggested by Sack, Maradudin & Weiss (930). However, to obtain  $\gamma_T$  between  $T = 0.2\Theta$  and  $T = 0$  one has to resort to direct numerical computation using specific models for the forces in the crystal lattice.

From the failure of convergence of the above series below  $0.2\Theta$ , Barron (64) predicted that the Grüneisen parameter  $\gamma_T$  must show a rapid change with temperature below  $T \approx 0.2\Theta$ . It was this prediction of Barron which stimulated a lot of experimental work on the thermal expansion of crystals down to liquid helium temperature because for most of the crystals this rapid change in  $\gamma_T$  should be expected in the liquid hydrogen temperature region.

Grüneisen (415) stated his law that  $\beta V/\chi_T C_v$  is constant, independent of temperature. This law is found to be approximately valid at moderately high temperatures. Grüneisen's law would be strictly valid at all temperatures if the Grüneisen parameters  $\gamma_{ji}$  for all the modes of lattice vibration were equal. This is improbable. In fact even for the simple Debye model of an isotropic elastic continuum, the longitudinal and transverse elastic waves would have different Grüneisen parameters leading to a temperature dependence of  $\gamma_T$  (Bijl & Pullan, 100). However, equality of  $\alpha$  the Grüneisen parameters is not necessary for a solid to obey Grüneisen's law. Blackman (106) has pointed out that the variation of  $\gamma_T$  can be considered from a different point of view. One constructs constant frequency surfaces  $\omega$  and  $\omega + d\omega$  in the Brillouin zone. The average Grüneisen parameter  $\bar{\gamma}(\omega)$  is defined by taking the average of the Grüneisen parameters of the individual modes in this frequency region.  $\gamma_T$  can now be redefined as

$$\gamma_T = \frac{\int_0^{\omega_m} \bar{\gamma}(\omega) \cdot \sigma(\omega) \cdot G(\omega) \cdot d\omega}{\int_0^{\omega_m} \sigma(\omega) \cdot G(\omega) \cdot d\omega} \quad (3.1.23)$$

where  $\sigma(\omega)$  is the Einstein specific heat function and  $G(\omega)$  is the frequency distribution function for the lattice. Though the individual Grüneisen parameters  $\gamma_{ji}$  for the different normal modes may be widely different, the average  $\bar{\gamma}(\omega)$  may not depend strongly on the frequency. This is the reason why  $\gamma_T$  shows a much smaller range of variation than the  $\gamma_{ji}$ .